Biochemical Pharmacology 81 (2011) 91–103

Contents lists available at ScienceDirect

Biochemical Pharmacology

journal homepage: www.elsevier.com/locate/biochempharm

The platinum (II) complex [Pt(O,O′-acac)(γ-acac)(DMS)] alters the intracellular calcium homeostasis in MCF-7 breast cancer cells

Antonella Muscella [a], Nadia Calabriso [b], Carla Vetrugno [b], Francesco Paolo Fanizzi [c], Sandra Angelica De Pascali [c], Carlo Storelli [b], Santo Marsigliante [b,*]

[a] Cell Pathology Lab, Dipartimento di Scienze e Tecnologie Biologiche e Ambientali (Di.S.Te.B.A.), Universitá di Lecce, Italy
[b] Cell Physiology Lab, Dipartimento di Scienze e Tecnologie Biologiche e Ambientali (Di.S.Te.B.A.), Universitá di Lecce, Italy
[c] General and Inorganic Chemistry Lab, Dipartimento di Scienze e Tecnologie Biologiche e Ambientali (Di.S.Te.B.A.), Universitá di Lecce, Italy

ARTICLE INFO

Article history:
Received 16 July 2010
Accepted 13 September 2010

Keywords:
[Pt(O,O′-acac)(γ-acac)(DMS)]
[Ca2+]i homeostasis
PMCA
PKC-α
ROS
MCF-7
ATP

ABSTRACT

It was previously demonstrated that [Pt(O,O′-acac)(γ-acac)(DMS)] exerted toxic effects at high doses, whilst sub-cytotoxic concentrations induced anoikis and decreased cell migration. Aim of this study was to investigate the hypothesis that [Pt(O,O′-acac)(γ-acac)(DMS)] alters the $[Ca^{2+}]_i$ and that this is linked to its ability to trigger rapid apoptosis in MCF-7 cells. Thus, cells were treated with [Pt(O,O′-acac)(γ-acac)(DMS)] and its effects on some of the systems regulating Ca^{2+} homeostasis were studied, also in cells dealing with the complex changes occurring during the Ca^{2+} signalling evoked by extracellular stimuli. [Pt(O,O′-acac)(γ-acac)(DMS)] caused the decrease of PMCA activity (but not SERCA or SPCA) and Ca^{2+} membrane permeability. These two opposite effects on $[Ca^{2+}]_i$ resulted in its overall increase from 102 ± 12 nM to 250 ± 24 nM after 15 min incubation. The effects of [Pt(O,O′-acac)(γ-acac)(DMS)] were also evident when cells were stimulated with ATP: the changes in Ca^{2+} levels caused by purinergic stimulation resulted altered due to decreased PMCA activity and to the closure of Ca^{2+} channels opened by purinergic receptor. Conversely, [Pt(O,O′-acac)(γ-acac)(DMS)] did not affect the store-operated Ca^{2+} channels opened by thapsigargin or by ATP. [Pt(O,O′-acac)(γ-acac)(DMS)] provoked the activation of PKC-α and the production of ROS that were responsible for the Ca^{2+} permeability and PMCA activity decrease, respectively. The overall effect of [Pt(O,O′-acac)(γ-acac)(DMS)] is to increase the $[Ca^{2+}]_i$, an effect that is likely to be linked to its ability to trigger rapid apoptosis in MCF-7 cells. These data reinforce the notion that [Pt(O,O′-acac)(γ-acac)(DMS)] would be a promising drug in cancer treatment.

1. Introduction

Free intracellular Ca^{2+}, acting as a second messenger, is crucial for a diverse range of biological functions, such as fertilization, neurotransmission, muscle contraction, and gene transcription [1]. Intracellular Ca^{2+} signalling is also a key regulator of proliferation [2], cell cycle progression [3], and apoptosis [4].

Although the essential role of Ca^{2+} signalling in maintaining homeostatic functions is well established, less is known about the role of aberrant Ca^{2+} signalling in disease [5,6]. In the past decade there has been a realization that particular cancers are associated with alterations in specific Ca^{2+} channels or pumps. Ca^{2+} signalling is involved in various tumorigenic pathways, and the inhibition or activation of specific Ca^{2+} channels or pumps can reduce cellular proliferation and/or induce apoptosis. There is an increasing awareness that PMCA alterations, concurrent with an increase in Ca^{2+} influx channel expression and TRPV6 [7], are associated with tumorigenesis, including that of the mammary gland [8]. Indeed, relative PMCA1 mRNA expression is greater in tumorigenic breast cancer MCF-7 and MDA-MB-231 cells than that in non-tumorigenic MCF-10A cells [9]. PMCA1 and PMCA4 expression is also lower in simian virus 40-transformed human skin fibroblasts [10]. Thus, perturbed PMCA regulation or function may be important in diseases such as cancer. Therapeutic modulation of PMCA expression and/or activity may have functional consequences in suppressing the tumorigenic phenotype. The appropriateness of PMCA as a possible drug target is also demonstrated by the prominence of other clinically used inhibitors of P-type ATPases, digoxin and omeprazole, as inhibitors of Na^+/K^+-ATPase and H^+/K^+-ATPase, respectively [11,12]. There are also studies indicating that modulators of Ca^{2+} signalling may offer an effective cell death induction and confer another layer of selectivity for cancer cells with an aberration in multiple Ca^{2+} channels or pumps. For

Abbreviations: CCE, capacitative calcium entry; DMEM, Dulbecco's modification of Eagle's medium; DMS, dimethylsulphide; ECL, enhanced chemiluminescence; NBT, nitroblue tetrazolium; PBS, phosphate-buffered saline; PKC-α, protein kinase C-alpha; PMCA, plasma membrane calcium ATPase; PVDF, polyvinylidene difluoride membrane; ROS, reactive oxygen species; SDS, sodium dodecyl sulphate.

* Corresponding author. Tel.: +39 0832 298 711; fax: +39 0832 324 220.
E-mail addresses: fp.fanizzi@unisalento.it (F.P. Fanizzi), santo.marsigliante@unile.it (S. Marsigliante).

0006-2952/$ – see front matter © 2010 Elsevier Inc. All rights reserved.
doi:10.1016/j.bcp.2010.09.012

example, tamoxifen alters Ca^{2+} signalling in MCF-7 breast cancer cells, and in malignant glioma cell lines it increases cytosolic Ca^{2+} responses to ATP-agonist activation [13]. In glioma cells tamoxifen also increases the radius of Ca^{2+} wave propagation and the rate of Ca^{2+} ionophore-mediated cell death.

Recently, this group has synthesized and studied a platinum complex containing two acetylacetonate (acac) ligands, one O,O′-chelate and the other sigma-linked by methionine in gamma position, and dimethyl-sulphide (DMS) in the metal coordination sphere, that has shown interesting biological activities [14]. This compound ([Pt(O,O′-acac)(γ-acac)(DMS)]) not only was able to induce apoptosis in endometrial cancer cells (HeLa), with activity up to about 100 times higher than that of cisplatin, but also showed high cytotoxicity in cisplatin resistant MCF-7 breast cancer cells. Differently from cisplatin, for which the activity appears to be associated both with its intracellular accumulation and with the formation of DNA adducts [15,16], the cytotoxicity of this new compound is related to the intracellular accumulation only, showing a low reactivity with nucleobases and a specific reactivity with sulphur ligands, suggesting that the cellular targets could be amino acid residues of proteins.

The different action mechanism of the new complex, having different biological targets, with respect to cisplatin, may render it intrinsically able to evoke less chemo-resistance phenomena. Here we wanted to see whether [Pt(O,O′-acac)(γ-acac)(DMS)] was able to increase the level of free $[Ca^{2+}]_i$ in fura-2-loaded MCF-7 cells. The $[Ca^{2+}]_i$ increase was characterized and the underlying mechanisms were investigated; this study indicates that [Pt(O,O′-acac)(γ-acac)(DMS)] alters the homeostasis of Ca^{2+} thus offering further therapeutic opportunities.

2. Materials and methods

2.1. Determination of $[Ca^{2+}]_i$

The medium was aspirated, and the cells were then harvested with 0.05% trypsin-EDTA solution. After washing the cells three times by pelleting ($100 \times g$ for 5 min), the cells (4×10^6) were incubated with 5 μM fura 2-AM and 0.2% pluronic F-127 for 45 min at 37 °C with continuous shaking (100 cycles/min). Following the loading period, the cells were washed twice with a modified Krebs–Ringer buffer in which the bicarbonate was replaced by 20 mM Hepes, pH 7.4, incubated again for at least 10 min at room temperature to facilitate hydrolysis of the esterified probe, and washed once again. The cells were resuspended in 2 ml of the same buffer containing 0.1% BSA, and 20 μl of the cell suspension was added to a 2 ml fluorescence cuvette kept at 37 °C, and stirred throughout the experiment. The fluorescence intensity was measured with a JASCO FP 750 fluorimeter (Jasco Corporation, Japan). The excitation wavelengths were 340 and 380 nm, and emission was measured at 510 nm. The maximal fluorescence was determined at the end of the assay by adding 20 μl 10% SDS and the minimal fluorescence by adding 20 μl 0.5 M EGTA solution, pH 9.0. The cytoplasmic Ca^{2+} concentration at the time t was calculated using the software of the fluorimeter and assuming a dissociation constant for the fura 2-Ca^{2+} complex of 224 nM, according to the Grynkiewicz equation [17]. Mn^{2+} strongly quenched the fura-2 fluorescence at 360 nm. Results are expressed as relative fluorescence quenching with respect to the maximal quenching induced by the addition of digitonin (80 μg/ml).

2.2. Ca^{2+}-ATPase activity measurement

ATPase activities were determined by measuring inorganic phosphate (Pi) production by the method of Fiske and Subarrow [18]. This method is based on the reaction between phosphate and molybdate, producing yellow molybdate phosphoric acid which contains a Mo(VI) that is then reduced to Mo(V) present in a blue-coloured heteropolyacid compound. This blue compound is directly measured by reading the absorbance at 700 nm. Ca^{2+}-dependent ATPase was measured in crude MCF-7 cell homogenates in the presence of 0.5 mM ouabain and 5 mM sodium azide, potent inhibitor of mitochondrial Ca^{2+} uptake. Typically, 100 μg total cell lysates were incubated for 10 min at 37 °C in a reaction mixture consisting of (in mM): 100 NaCl, 20 KCl, 15 Hepes, 12 Tris, 1.2 $MgCl_2$, 2.5 ATP. This reaction buffer was supplemented with 200 μM $CaCl_2$ and the free Ca^{2+} concentration (3 μM) has been calculated using the CHELATOR program (BMAXC STANDARD, http://www.stanford.edu). The further addition of 1 μM of thapsigargin (to inhibit SERCA activity, [19]), and of 2 μM orthovanadate (a dose used to selectively inhibit PMCA activity freshly prepared to avoid its transformation to decameric vanadate species, [20]) and of 800 μM EGTA (to measure the Mg^{2+}-ATPase activity) were made in three different steps, and the activity was measured after each addition in order to evaluate the contribution of each ATPase to the total ATPase activity. The total Ca^{2+}-ATPase activity (i.e., the sum of SERCA, PMCA, and SPCA) was obtained after subtraction of the Mg^{2+}-ATPase activity from the (Ca^{2+} + Mg^{2+})-ATPase activity obtained immediately after the addition of ATP. The SERCA activity was calculated by subtracting the activity measured in the presence of thapsigargin (which includes PMCA, SPCA, and Mg^{2+}-ATPase activities) from the total (Ca^{2+} + Mg^{2+})-ATPase activity. The SPCA activity was calculated by subtracting the Mg^{2+}-ATPase activity from the activity in the presence of thapsigargin and vanadate. The PMCA activity was calculated by subtracting the Mg^{2+}-ATPase activity and the SPCA activity from the activity in the presence of thapsigargin. Comparable results were obtained when PMCA activity was measured by using carboxyeosin, frequently mentioned as PMCA inhibitor [21].

2.3. Preparation of subcellular fraction

To obtain protein cell extracts and subcellular fractions we used a procedure previously described [22]. Cells were washed twice in ice-cold PBS and harvested in 1 ml of PBS. The samples were centrifuged for 30 s at $10{,}000 \times g$, and cell pellets were resuspended in the following buffer (mM): 20 Tris–HCl, pH 8.0, containing 100 NaCl, 2 EDTA, 2 Na_3VO_4, 0.2% Nonidet P-40 and 10% glycerol, supplemented with a cocktail of protease inhibitors. After a 10 min incubation on ice, cells were passed several times through a 20 gauge syringe and then centrifuged at $13{,}000 \times g$ for 10 min at 4 °C. For preparation of subcellular fractions cells were ruptured in homogenization buffer (mM): 20 Tris HCl, pH 7.5, containing 250 sucrose, 2 EDTA, 0.5 EGTA, 0.2 phenylmethylsulphonyl fluoride and a cocktail of protease inhibitors, by Dounce homogenization and centrifuged immediately at $2{,}000 \times g$ for 10 min. The supernatant was collected and centrifuged at $100{,}000 \times g$ for 1 h to separate cytosolic and membrane fractions. The membrane fraction was subsequently resuspended in extraction buffer (mM): 20 Tris HCl, pH 7.5, containing 150 NaCl, 1 EDTA, 1 EGTA, and a cocktail of protease inhibitors (containing 0.2 mM phenylmethylsulphonyl fluoride, 10 μg/ml aprotinin, 10 μg/ml soybean trypsin inhibitor and 10 μg/ml leupeptin) with 1% (vol/vol) Nonidet P-40. Nuclei were pelleted by centrifugation at $2{,}000 \times g$ for 15 min at 4 °C and resuspended in high-salt buffer (mM): 20 Tris–HCl, pH 7.9, 420 NaCl, 10 KCl, 0.1 Na_3VO_4, 1 EDTA, 1 EGTA, 20% glycerol, supplemented with a cocktail of protease inhibitors, and sonicated until no nuclei remained intact. Samples were then centrifuged at $13{,}000 \times g$ for 10 min at 4 °C, and the resultant supernatant was used as the nuclear extract. The purity of fractions was tested by immunoblotting with antibodies specific to α-Na^+/K^+ ATPase subunity (membrane protein) and β-actin (cytoplasmic protein). Proteins in the homogenates and cellular

fraction were determined using the Bio-Rad protein assay kit 1. Lyophilized bovine serum albumin was used as a standard.

2.4. Western blot analysis

Proteins in homogenates and cellular fraction were determined using the Bio-Rad protein assay kit 1 (Milan, Italy). Lyophilised bovine serum albumin was used as a standard. Total cell proteins or proteins of the distinct subcellular fractions were dissolved in SDS sample buffer and separated on 10% or 15% SDS gels. Separated proteins were transferred electrophoretically onto polyvinylidene difluoride membrane (PVDF) (Amersham International). Equal protein loading was confirmed by Ponceau S staining. Blots were incubated with specific primary antibodies and the immune complexes were detected using appropriate peroxidase conjugated secondary antibodies and enhanced chemiluminescent detection reagent ECL (Amersham International). Blots were stripped and used for sequential incubations with relative control antibody (α-Na^+/K^+ATPase subunity for membrane protein and β-actin for cytoplasmic protein). Densitometric analysis was carried out on Western blots using the NIH Image (v1.63) software. The pixel intensity for each region was analyzed, the background was subtracted, and the protein expressions were normalized to β-actin loading control for each lane.

2.5. Intracellular reactive oxygen species (ROS) formation

ROS generation was detected by nitroblue tetrazolium (NBT) assay as previously described [22]. NBT (1 mg/ml) was added to medium of treated MCF-7 and incubations were carried out at 37 °C for 15–60 min. NBT is reduced by ROS to a dark blue insoluble form of NBT called formazan. Cells were then carefully washed and lysed in a 90% dimethylsulphoxide solution containing 0.01 N NaOH and 0.1% SDS. Absorbance of formazan was measured at 550 nm against lysis buffer blank. Data are expressed as % of control untreated MCF-7 cells.

2.6. Anion superoxide ($O_2^{\bullet-}$) production

$O_2^{\bullet-}$, the main free radical produced in mitochondria, was measured using the cell-permeable probe MitoSOX Red. The reduced probe is taken up by cells and in the presence of $O_2^{\bullet-}$ is oxidized and becomes fluorescent, emitting a red fluorescence after 488 nm laser excitation. After treatment with the drug, cells were incubated for 10 min with MitoSOX Red reagent 5 μM in 0.5 ml of Hank's Balanced Salt Solution with calcium and magnesium ($CaCl_2$ 140 mg/l, $MgCl_2$-$6H_2O$ 10 mg/l and $MgSO_4$-$7H_2O$ 10 mg/l) at 37 °C. After washing twice, adhered cells were observed (maximum excitation/emission of MitoSOX reagent: 510/580 nm) and images and values of fluorescence were obtained by fluorescence microscopy as mean fluorescence intensities (MFI/cell).

2.7. Statistical analysis

Experimental points represent means ± standard deviation (S.D.) of 3–6 replicates. Statistical analysis was carried out using the ANOVA. When indicated, post hoc tests (Bonferroni/Dunn) were also performed. A p value less than 0.05 was considered to achieve statistical significance.

2.8. Reagents and MCF-7 cell line

The PKC inhibitors GF109203X and Gö6976 were obtained from Calbiochem (Darmstadt, Germany). Fura 2-AM and thapsigargin were from Molecular Probes (Eugene, OR, USA). Antibodies used in western analyses to PKC-α, -ε, -δ, -ι and -ζ, β-actin and α-subunit of Na+/K+ATPase, goat anti-rabbit IgG conjugated with peroxidase, as well as control antibodies, were obtained from Santa Cruz Biotechnology (Santa Cruz, CA, USA). The inhibitors of NADPH oxidase, diphenyleneiodonium (DPI) and apocynin, nitroblue tetrazolium (NBT), MitoSOX Red and all the inorganic salts were obtained from Sigma (Milan, Italy).

MCF-7 cell line was cultured in DMEM (Celbio, Pero, Milan, Italy) supplemented with 10% fetal bovine serum, penicillin (100 U/ml) and streptomycin (100 mg/ml). Cells were grown to 70% confluence and then treated with [Pt(O,O′-acac)(γ-acac)(DMS)] at various concentrations and for different incubation periods.

3. Results

3.1. Effects of [Pt(O,O′-acac)(γ-acac)(DMS)] on $[Ca^{2+}]_i$

We showed previously that the new Pt complex containing an O,O′-chelated acetylacetonate ligand (acac) and a dimethylsulphide in the Pt coordination sphere, [Pt(O,O′-acac)(γ-acac)(DMS)], induces apoptosis in MCF-7 breast cancer cell line,

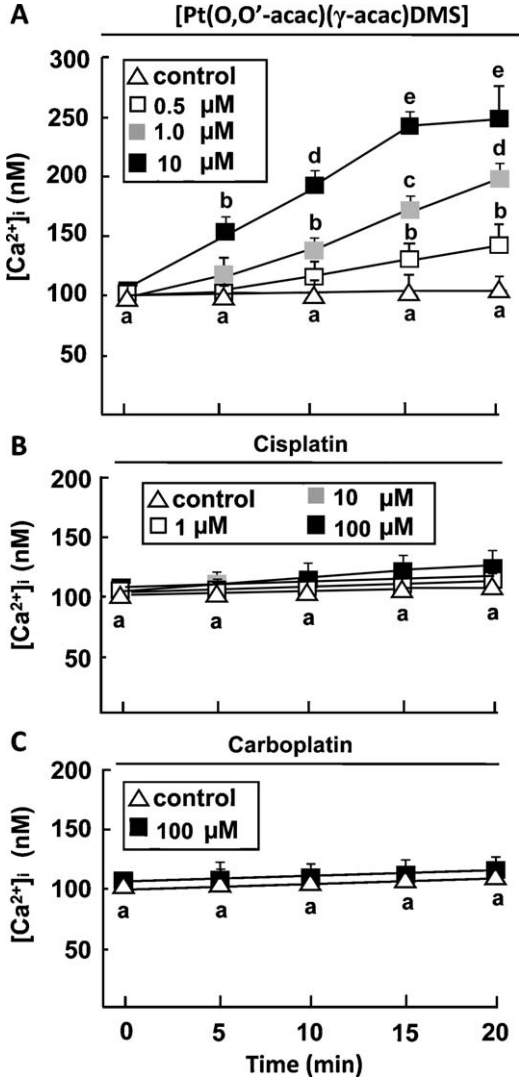

Fig. 1. Effects of Pt(II) compounds on $[Ca^{2+}]_i$.
Intracellular Ca^{2+} concentration was quantified by fluorescence after loading the cells with the calcium indicator fura-2-AM. Time-course of the effects of various concentrations of (A) [Pt(O,O′-acac)(γ-acac)(DMS)], (B) Cisplatin and (C) 100 μM Carboplatin on $[Ca^{2+}]_i$ in MCF-7 cells. Results shown are representative of six separate experiments. Values with shared letters are not significantly different according to Bonferroni/Dunn post hoc tests.

relatively insensitive to cisplatin. In contrast to cisplatin, the cytotoxicity of [Pt(O,O′-acac)(γ-acac)(DMS)] correlated with cellular accumulation but not with DNA binding, as it activates the mitochondrial apoptotic pathway [16]. In many cases, an early and pivotal event in apoptosis is a cytosolic free Ca^{2+} concentration ($[Ca^{2+}]_i$) increase. To determine whether this was an early event during [Pt(O,O′-acac)(γ-acac)(DMS)], induced apoptosis, we first examined whether intracellular $[Ca^{2+}]_i$ levels increased in MCF-7 cells after [Pt(O,O′-acac)(γ-acac)(DMS)] exposure, using fura-2-AM in a spectrofluorometric assay. In MCF-7 cells, the basal level of $[Ca^{2+}]_i$ was 102 ± 7 nM (mean ± S.D.; $n = 30$). MCF-7 cells were incubated for different times (1–20 min) with crescent concentrations of [Pt(O,O′-acac)(γ-acac)(DMS)]. The treatment with [Pt(O,O′-acac)(γ-acac)(DMS)] increases $[Ca^{2+}]_i$ in dose-dependent manner (Fig. 1A); between 0.5 and 10 μM, the increase in $[Ca^{2+}]_i$ ranged from 145 ± 10 nM to 250 ± 24 nM. Concentrations above 10 μM were not tested because they are clinically irrelevant. In MCF-7 cells, the increase in $[Ca^{2+}]_i$ was restricted to [Pt(O,O′-acac)(γ-acac)(DMS)] since cisplatin and carboplatin (up to a concentration of 100 μM), did not elevate $[Ca^{2+}]_i$ (Fig. 1B and C). While transient elevations of $[Ca^{2+}]_i$ are important signals within cells, prolonged elevations of $[Ca^{2+}]_i$ could be lethal. A $[Ca^{2+}]_i$ overload may activate cell death via apoptosis [4]. Theoretically, there are at least two possibilities for altering $[Ca^{2+}]_i$ homeostasis in MCF-7 cells by [Pt(O,O′-acac)(γ-acac)(DMS)]. Elevation of the $[Ca^{2+}]_i$ can result: a) from Ca^{2+}-influx from the extracellular space and/or from Ca^{2+}-release from intracellular stores; b) from Calcium-ATPases (PMCA/SERCA/SPCA) and/or the Na^+-Ca^{2+}-Exchanger (NCX) activity inhibition.

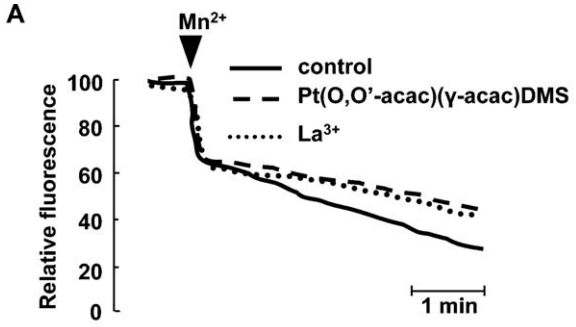

B

		ΔF_{360}·min^{-1}
Control		6.83 ± 0.32 [a]
0.5 μM	Pt(O,O'-acac)(γ-acac)DMS	4.79 ± 0.27 [b]
1.0 μM	Pt(O,O'-acac)(γ-acac)DMS	3.95 ± 0.24 [c]
10 μM	Pt(O,O'-acac)(γ-acac)DMS	2.19 ± 0.13 [d]
100 μM	La^{3+}	2.22 ± 0.19 [d]
100 μM	La^{3+} + 10 μM $Pt(acac)_2DMS$	2.16 ± 0.10 [d]

Fig. 2. Comparison of the permeabilities of the plasma membrane to Mn^{2+} in absence and in presence of [Pt(O,O′-acac)(γ-acac)(DMS)].
Mn^{2+} entry was measured by the quenching of fluorescence with an excitation wavelength of 360 nm, and an emission wavelength of 510 nm. The curves represent fluorescence relative to total quenching attained by the addition of digitonin to saturate fura-2 with Mn^{2+}. (A) Cells were kept in nominally Ca^{2+}-free medium, as 2 mM Mn^{2+} was applied to the medium (arrow), it entered cells, with Mn^{2+} entry much slower in [Pt(O,O′-acac)(γ-acac)(DMS)]-treated cells. Mn^{2+} entry was blocked by the impermeant cation La^{3+} (100 μM), and [Pt(O,O′-acac)(γ-acac)(DMS)] had, on Mn^{2+} influx, effects similar to those obtained by La^{3+}. Each tracing is representative of five separate experiments. (B) The permeability of MCF-7 cell plasma membrane was significantly decreased by [Pt(O,O′-acac)(γ-acac)(DMS)] in a dose-dependent manner. Mn^{2+} entry in cells treated with 10 μM [Pt(O,O′-acac)(γ-acac)(DMS)] was the same in the presence or in the absence of La^{3+}. Average data are from experiments shown in A ($n = 5$). Values with shared letters are not significantly different according to Bonferroni/Dunn post hoc tests. $Pt(acac)_2DMS$ stands for Pt(O,O′-acac)(γ-acac)DMS.

3.2. Effect of [Pt(O,O′-acac)(γ-acac)(DMS)] on Mn^{2+} uptake in MCF-7 cells

To test whether the changes of the $[Ca^{2+}]_i$ response caused by [Pt(O,O′-acac)(γ-acac)(DMS)] were due to modulation of the plasma membrane permeability, we measured Mn^{2+} influx after the addition of [Pt(O,O′-acac)(γ-acac)(DMS)]. Mn^{2+} is a good Ca^{2+}-entry tracer, since it is not pumped out of the cell [23]. Mn^{2+} uptake was estimated by the quenching of fura-2 fluorescence when excited at 360 nm, which is an isosbestic wavelength and is insensitive to variations in $[Ca^{2+}]_i$ concentration. Fig. 2A shows the fluorescence quenching by Mn^{2+} influx: the membrane permeability was significantly decrease by [Pt(O,O′-acac)(γ-acac)(DMS)] in a dose-dependent manner (Fig. 2B). Mn^{2+} entry was drastically decreased by the impermeant cation La^{3+} (100 μM), an effect similar to that obtained with 10 μM [Pt(O,O′-acac)(γ-acac)(DMS)] (Fig. 2). The effect of 10 μM [Pt(O,O′-acac)(γ-acac)(DMS)] or 100 μM La^{3+} on Mn^{2+} entry was not augmented were both were used in combination (Fig. 2B).

3.3. Inhibitory effects of [Pt(O,O′-acac)(γ-acac)(DMS)] on of Ca^{2+}-ATPases activity

First, Ca^{2+}-dependent ATPase was measured in crude MCF-7 cell homogenates in the presence of 0.5 mM ouabain. The method used to measure Ca^{2+}-dependent ATPase in MCF-7 cells was sensitive and reproducible. In standard culture conditions, the coefficient of variation of a single assay was 3.2% ($n = 8$) and Ca^{2+}-dependent ATPase activities (PMCA, SERCA and SPCA) increased linearly with increasing protein concentrations. Fig. 3A presents data on ouabain-insensitive ATP hydrolysis in the presence and absence (obtained adding 800 μM EGTA) of Ca^{2+}. MCF-7 cells clearly catalysed Ca^{2+}-sensitive ATP hydrolysis. Approximately 35% of ouabain-insensitive ATPase activity (~7.1 ± 0.3 μmol Pi/h/mg/protein as previously shown, [24]) was Ca^{2+}-dependent. This activity consisted of the following activities: PMCA (1.12 ± 0.11 μmol Pi/h/mg/protein), SERCA (0.63 ± 0.11 μmol Pi/h/mg/protein and SPCA (0.16 ± 0.13 μmol Pi/h/mg/protein) (all the activities were mean ± S.D. of five independent experiments, Fig. 3A). [Pt(O,O′-acac)(γ-acac)(DMS)] (0.1–10 μM) had no effects on SERCA activity (Fig. 3B), nor on that of the SPCA (data not shown). Conversely, [Pt(O,O′-acac)(γ-acac)(DMS)] produced a significant decrease in PMCA activity in a dose- and time-dependent manner (ANOVA: $P < 0.0001$; Fig. 3B and C). The maximal effect, in sub-confluent conditions, was obtained after 10 min of incubation with 10 μM [Pt(O,O′-acac)(γ-acac)(DMS)], and corresponded to a 1.6-fold decrement in PMCA activity.

3.4. Effects of [Pt(O,O′-acac)(γ-acac)(DMS)] on ATP-induced Ca^{2+} response in MCF-7 cells

In order to understand whether the effects provoked by [Pt(O,O′-acac)(γ-acac)(DMS)] had an effective role in controlling the homeostasis of intracellular calcium, we provoked physiological disturbances in $[Ca^{2+}]_i$ using ATP, an agonist able to induce intracellular calcium signalling in MCF-7 cells, due to stimulation of phospholipase C through P2Y2 receptors [25]. The $[Ca^{2+}]_i$ transient evoked by ATP consisted of a rapid peak followed by a sustained phase of elevated $[Ca^{2+}]_i$, which persisted for over 3 min (Fig. 4A). The maximum increase in $[Ca^{2+}]_i$ was observed at 100 μM ATP, with a $[Ca^{2+}]_i$ of 509 ± 21 nM. ATP-induced $[Ca^{2+}]_i$ transients were then examined in the presence of increasing [Pt(O,O′-acac)(γ-acac)(DMS)] concentrations (0.5–10 μM). As shown in

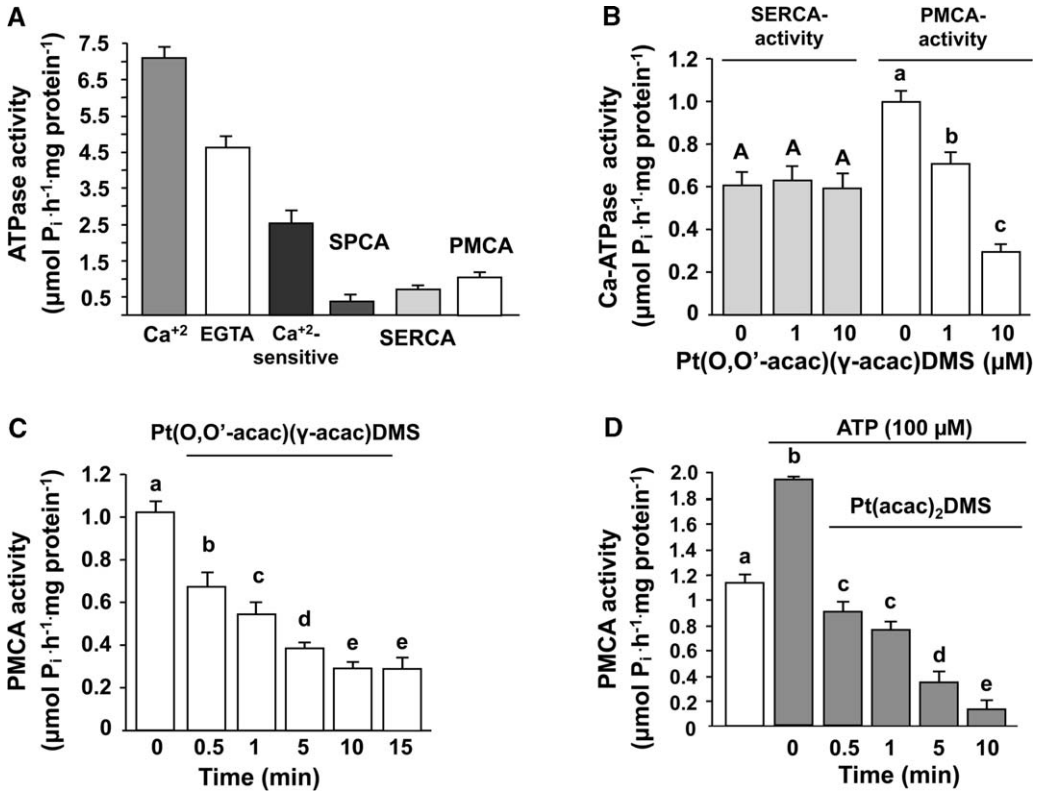

Fig. 3. Effects of [Pt(O,O′-acac)(γ-acac)(DMS)] on Ca^{2+}-ATPases activities.
(A) ATPase activity was assessed in the presence of 0.5 mM ouabain, as inorganic phosphate (Pi) liberated from ATP during a 10 min incubation at 37 °C. Ca^{2+} refers to incubation in the presence of 80 μM $CaCl_2$, while EGTA refers to incubation with 800 μM EGTA. Ca^{2+}-sensitive ATPase activity is the difference between the two conditions. In order to identify the relative contributions of the PMCA, SPCA and SERCA, Ca^{2+}-sensitive ATPase activity was assessed in the presence of the SERCA inhibitor thapsigargin or/and in presence of eosin and orthovanadate, as detailed in Section 2. The Ca^{2+}-ATPase activities were expressed as μM of Pi liberated per mg of protein per hour, based on values from a standard curve of the absorbance using various concentrations of free Pi.
(B) MCF-7 cells were stimulated or not with 0.5 or 10 μM [Pt(O,O′-acac)(γ-acac)(DMS)] for 10 min, and then SERCA and PMCA activities were assessed.
(C) Effects of increasing incubation times of 10 μM [Pt(O,O′-acac)(γ-acac)(DMS)] on PMCA activity in MCF-7 cells.
(D) MCF-7 were stimulated with ATP (100 μM) for 2.5 min; afterwards, [Pt(O,O′-acac)(γ-acac)(DMS)] (10 μM) was added for the indicated times in order the assess its effects on the effects induced by ATP on the PMCA activity. The data are means ± S.D. of four different experiments run in triplicate. Values with shared letters are not significantly different according to Bonferroni/Dunn post hoc tests. $Pt(acac)_2$DMS stands for Pt(O,O′-acac)(γ-acac)DMS.

Fig. 4A, in a first phase lasting about 1 min, 10 μM [Pt(O,O′-acac)(γ-acac)(DMS)] significantly decreased the peak of $[Ca^{2+}]_i$ (from 509 ± 21 nM to 440 ± 18 nM, $n = 7$; $p < 0.001$); afterwards, it increased, in a dose-dependent manner, both the rate of the Ca^{2+} decline and the post-stimulatory $[Ca^{2+}]_i$ level, calculated after 3 min from ATP administration. In order to quantify the effect of [Pt(O,O′-acac)(γ-acac)(DMS)] on such ATP-evoked Ca^{2+} transient, the variations in Ca^{2+} profile were also evaluated both as *b*/*a* ratio and as Ca^{2+} rate of decline. Precisely, we expressed the $[Ca^{2+}]_i$ observed after 2 min from stimulation (*b*), as a fraction of $[Ca^{2+}]_i$ peak (*a*) (Fig. 4B *inset*), and the *b*/*a* ratio was calculated for the different concentrations (0.5–10 μM). Fig. 4B shows that under control conditions (i.e., exposure to ATP alone) (*b*) was 30% of peak $[Ca^{2+}]_i$. When applied together with ATP, [Pt(O,O′-acac)(γ-acac)(DMS)] increased, in a dose dependent manner, the *b*/*a* ratio (Fig. 4B). The effect provoked by the channel blocker La^{3+} (100 μM), was very different from the effect of 10 μM [Pt(O,O′-acac)(γ-acac)(DMS)] (Fig. 4B and C), inasmuch as, while they both were able to strongly reduce the Ca^{2+} entry, La^{3+}, differently from [Pt(O,O′-acac)(γ-acac)(DMS)], had no effect on PMCA activity. This suggests that the increase in the *b*/*a* ratio caused by [Pt(O,O′-acac)(γ-acac)(DMS)] is mainly due to inhibition of the pump rather than the decrease of plasma membrane permeability. Obviously, [Pt(O,O′-acac)(γ-acac)(DMS)]-treated cells had a slower rate of PMCA-mediated free intracellular Ca^{2+} efflux. The rate of decline, assayed in a time interval of 1 min after the peak, could be a relative measure of PMCA-mediated free intracellular Ca^{2+} efflux. The rates of decline in $[Ca^{2+}]_i$ obtained with the various [Pt(O,O′-acac)(γ-acac)(DMS)] concentrations were plotted against the relative $[Ca^{2+}]_i$ peak values, for comparisons of PMCA-mediated Ca^{2+} efflux rates (Fig. 4D). In order to discriminate between the effects on plasma membrane channels and PMCA inhibition provoked by [Pt(O,O′-acac)(γ-acac)(DMS)] and those due to the channel closure only, the rate of decline in $[Ca^{2+}]_i$ obtained with 100 μM La^{3+} was also evaluated; as shown in Fig. 4D, La^{3+} provoked a rate of Ca^{2+} decline and a Ca^{2+} peak value significantly different from those provoked by [Pt(O,O′-acac)(γ-acac)(DMS)]. Since PMCA activity is known to be Ca^{2+}-dependent, MCF-7 cells were treated or not, for the indicated times, with 100 μM ATP and then Ca^{2+}-ATPase activity was assayed. ATP stimulated PMCA activity by about 50% after 2.5 min incubation and [Pt(O,O′-acac)(γ-acac)(DMS)] significantly decreased the activity of the ATP-stimulated PMCA (Fig. 3D). The origin of the ATP-induced Ca^{2+} sustained phase was studied using a Ca^{2+}-free medium obtained substituting 2 mM $MgCl_2$ for 2 mM $CaCl_2$ in the standard experimental medium previously passed through a Chelex 100 column. In these experimental conditions, the effect of ATP on peak height was much less pronounced with respect to that obtained in the presence of Ca^{2+}-containing solution ($[Ca^{2+}]_i$ peak decreased from 509 ± 21 nM to 286 ± 12 nM ($p < 0.001$). Fig. 5A shows an example of a $[Ca^{2+}]_i$ transient evoked by bath application of ATP (100 μM) in Ca^{2+}-free external solution. The ATP-induced $[Ca^{2+}]_i$ transient was characterized by a rapid and pronounced initial rise that then declined completely to the pre-stimulatory level. When ATP was applied

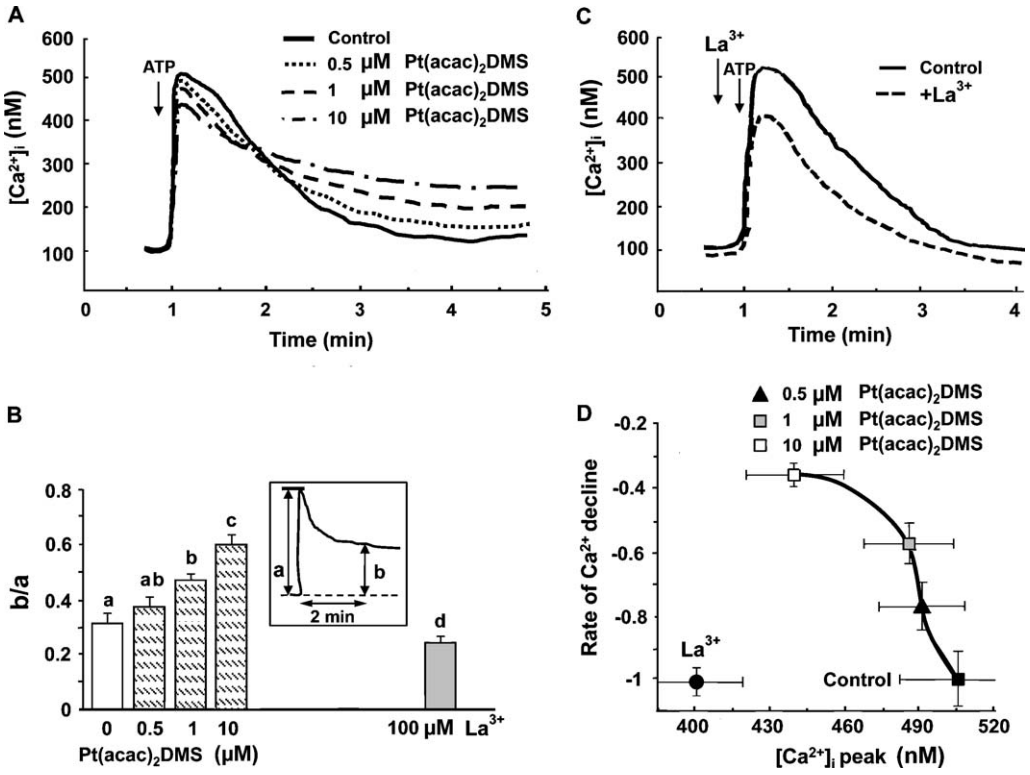

Fig. 4. Effects of [Pt(O,O′-acac)(γ-acac)(DMS)] and La^{3+} on the ATP-induced Ca^{2+} transients.
(A) MCF-7 cells, loaded with fura-2-AM, were stimulated with 100 μM ATP in the presence of extracellular Ca^{2+}. The effects of ATP on $[Ca^{2+}]_i$ were also assessed in the presence of increasing concentrations of [Pt(O,O′-acac)(γ-acac)(DMS)]. Each tracing is representative of seven separate experiments.
(B) Inhibitory action of [Pt(O,O′-acac)(γ-acac)(DMS)] on ATP-induced $[Ca^{2+}]_i$ transients was quantified by the *b*/*a* ratio, in which *a* represents the maximum peak amplitude (see *B*, *inset*) and *b* is the amplitude of the sustained component evaluated after 2 min from ATP administration. The *b*/*a* ratio was calculated for [Pt(O,O′-acac)(γ-acac)(DMS)], and for 100 μM La^{3+}, and then plotted for the various concentrations of [Pt(O,O′-acac)(γ-acac)(DMS)]. Each bar represents mean ± S.D. of seven separate experiments. Values with shared letters are not significantly different according to Bonferroni/Dunn post hoc tests.
(C) Effect of lanthanum on ATP-mediated $[Ca^{2+}]_i$ increases in MCF-7 cells; cells were incubated with 100 μM ATP or pre-treated with 100 μM La^{3+} for 30 s prior stimulation with 100 μM ATP. Each tracing is representative of seven separate experiments.
(D) The rate of decline of $[Ca^{2+}]_i$ transient assayed in a time interval of 1 min after the peak, is a relative measure of PMCA-mediated free intracellular Ca^{2+} efflux. The rates of decline in $[Ca^{2+}]_i$ obtained with the various [Pt(O,O′-acac)(γ-acac)(DMS)] concentrations and with 100 μM La^{3+} were plotted against the relative $[Ca^{2+}]_i$ peak values for comparisons of PMCA-mediated Ca^{2+} efflux rates in [Pt(O,O′-acac)(γ-acac)(DMS)]-treated and non MCF-7 cells. $Pt(acac)_2DMS$ stands for Pt(O,O′-acac)(γ-acac)DMS.

simultaneously with [Pt(O,O′-acac)(γ-acac)(DMS)], the $[Ca^{2+}]_i$ transient appeared significantly wide and decelerated (Fig. 5B). In MCF-7 cells, the pathway that links purinoceptors to intracellular Ca^{2+} release involves the InsP3 signalling cascade [26]; such Ca^{2+} release then results in external Ca^{2+} entry. Thus, we investigated whether the InsP3-dependent Ca^{2+} release was involved in the [Pt(O,O′-acac)(γ-acac)(DMS)]-induced $[Ca^{2+}]_i$ increase by using 2-aminoethoxydiphenyl borate (2-APB), a membrane-permeant InsP3R blocker [27]. Cells incubated with 20 μM 2-APB 10 min before the stimulation with 100 μM ATP, in Ca^{2+}-free conditions, led to a significant reduction (by 62 ± 6%, $n = 5$, $P < 0.05$) of the amplitude of the ATP-induced $[Ca^{2+}]_i$ transient (Fig. 5A and C), confirming prior observations showing that the ATP induced $[Ca^{2+}]_i$ transient is due to Ca^{2+} release through InsP3Rs [28]. Afterwards, cells were incubated with 20 μM 2-APB for 10 min and then stimulated with ATP together with [Pt(O,O′-acac)(γ-acac)(DMS)]: again, a significant inhibition of the $[Ca^{2+}]_i$ transient (by 68 ± 5%, $n = 5$, $P < 0.05$) was obtained (Fig. 5B and C), similar to that obtained in the absence of [Pt(O,O′-acac)(γ-acac)(DMS)], therefore suggesting that [Pt(O,O′-acac)(γ-acac)(DMS)] caused an InsP3-independent Ca^{2+} increase. Extracellular Ca^{2+} entry was generated by adding 2 mM $CaCl_2$ to the Ca^{2+}-free buffer after recovery of the ATP-induced $[Ca^{2+}]_i$ transient. The combined administration of ATP and [Pt(O,O′-acac)(γ-acac)(DMS)] (10 μM) reduced from 284 ± 10 nM to 265 ± 9 nM ($p < 0.001$; $n = 6$) the peak height of extracellular Ca^{2+} entry (Fig. 5B). 2-APB (20 μM) completely abolished the extracellular Ca^{2+} entry in cells stimulated with ATP alone or with ATP plus [Pt(O,O′-acac)(γ-acac)(DMS)] (Fig. 5).

3.5. Effect of [Pt(O,O′-acac)(γ-acac)(DMS)] on thapsigargin-evoked extracellular Ca^{2+} entry

Thapsigargin, an inhibitor of the SERCA, allows Ca^{2+} to leak out from the ER pool [19] causing complete store depletion also in MCF-7 cells [29]. The simultaneous administration of thapsigargin and [Pt(O,O′-acac)(γ-acac)(DMS)] to MCF-7 cells, kept in Ca^{2+}-free medium, increased the $[Ca^{2+}]_i$ peak, probably as a consequence of the decreased PMCA activity (Fig. 6B and C). In fact, a similar $[Ca^{2+}]_i$ increase was also obtained by pretreatment of cells with orthovanadate ($[VO_3(OH)]_2$), a PMCA inhibitor [20] (Fig. 6B and C). Furhermore, differences in extracellular Ca^{2+} entry obtained by thapsigargin, in the presence and in the absence of [Pt(O,O′-acac)(γ-acac)(DMS)], were also observed (Fig. 6B and D). However, the effects of [Pt(O,O′-acac)(γ-acac)(DMS)] on extracellular Ca^{2+} entry due to ATP or thapsigargin were different (Fig. 6A and D). The effects of [Pt(O,O′-acac)(γ-acac)(DMS)] on the extracellular Ca^{2+} entry were also evaluated by using the Mn^{2+} quenching technique, since this cation is not transported by the major calcium pumps, SERCA and PMCA. Indeed, the entry of Mn^{2+} increased in both thapsigargin- and ATP-treated cells, resulting however significantly higher when using ATP (Fig. 6 E and F), probably because of the opening of second messengers-operated Ca^{2+} channels, in addition to store-operated channels. When 10 μM [Pt(O,O′-acac)(γ-acac)(DMS)] was administered together with thapsigargin or ATP, the quenching of Mn^{2+} significantly decreased, reaching the same value (Fig. 6F). Taken together, these results suggest that the

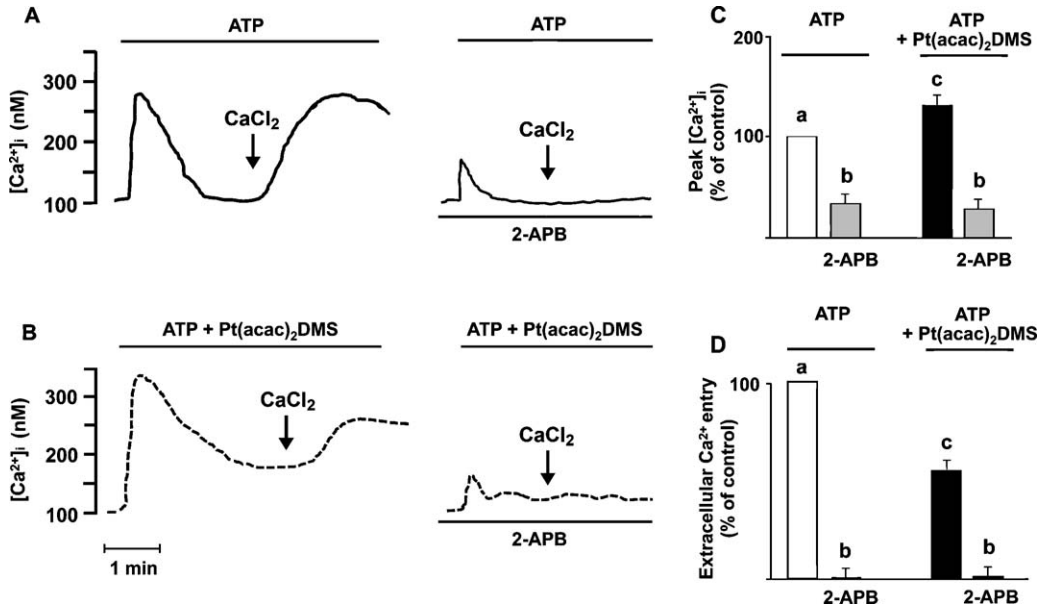

Fig. 5. Effect of 2-aminoethoxydiphenyl borate (2-APB) on ATP- and ATP plus [Pt(O,O′-acac)(γ-acac)(DMS)]-induced intracellular Ca^{2+} release and extracellular Ca^{2+} entry. (A, B) 2-APB (20 μM), a membrane-permeant InsP3R blocker, was applied to MCF-7, kept in nominal Ca^{2+}-free medium, 10 min before the stimulation with 100 μM ATP (A) or the co-stimulation with ATP and 10 μM [Pt(O,O′-acac)(γ-acac)(DMS)] (B). 2-APB caused a significant inhibition of the ATP-induced intracellular Ca^{2+} release both in the absence and in the presence of 10 μM [Pt(O,O′-acac)(γ-acac)(DMS)]. Afterwards, 2 mM $CaCl_2$ was added in order to assess the extracellular Ca^{2+} entry. Example traces of $[Ca^{2+}]_i$ induced transients are shown.
(C, D) Summary of the effects of 2-APB on ATP- and ATP + [Pt(O,O′-acac)(γ-acac)(DMS)]-induced Ca^{2+} release (C) and extracellular Ca^{2+} entry (D). Data are presented as average percentages ± S.D. of control (ATP, open bar; [Pt(O,O′-acac)(γ-acac)(DMS)], solid bar), i.e., the amplitude of the Ca^{2+} peak (C) and of extracellular Ca^{2+} entry (D) measured in the absence of 2-APB. The data are means ± S.D. of five different experiments. Values with shared letters are not significantly different according to Bonferroni/Dunn post hoc tests. $Pt(acac)_2DMS$ stands for [Pt(O,O′-acac)(γ-acac)DMS].

Ca^{2+}/Mn^{2+}-permeable plasma membrane channels opened by ATP only are targets of [Pt(O,O′-acac)(γ-acac)(DMS)]. Conversely, the Ca^{2+}/Mn^{2+}-permeable plasma membrane store-operated channels opened by both ATP and thapsigargin, may not be affected by [Pt(O,O′-acac)(γ-acac)(DMS)].

3.6. Effects of [Pt(O,O′-acac)(γ-acac)(DMS)] on Na^+/Ca^{2+}-exchanger activity

In order to understand the involvement of a Na^+/Ca^{2+} exchanger in the [Pt(O,O′-acac)(γ-acac)(DMS)]-induced $[Ca^{2+}]_i$ changes, we studied the effects of [Pt(O,O′-acac)(γ-acac)(DMS)] on Ca^{2+} influx using buffers with Na^+ concentrations being 0 and 140 mM. First, the effects of ATP were dependent on Na^+ concentration, since the replacement of extracellular Na^+ with choline, significantly increased the early peak rise in $[Ca^{2+}]_i$ from 509 ± 21 nM to 585 ± 30 nM (ANOVA; $p < 0.001$; $n = 6$, Fig. 7A). Secondly, cells co-stimulated with ATP and [Pt(O,O′-acac)(γ-acac)(DMS)], displayed a lower $[Ca^{2+}]_i$ peak in the presence of 140 mM Na^+ (450 ± 15 nM, $n = 6$) than in the absence (525 ± 21 nM, $n = 6$, Fig. 7B). Since the difference between the early peak rise in $[Ca^{2+}]_i$ obtained in physiological and Na^+-free buffers in the absence or presence of [Pt(O,O′-acac)(γ-acac)(DMS)] is practically identical (Fig. 7C), we may conclude that [Pt(O,O′-acac)(γ-acac)(DMS)] has no effects on the activity of the Na^+/Ca^{2+} exchanger.

3.7. Effects of [Pt(O,O′-acac)(γ-acac)(DMS)]-activated PKC-α on extracellular Ca^{2+} entry

Protein kinase C (PKC) is known to regulate Ca^{2+} homeostasis through negative feedback mechanisms [30]. Inasmuch as activated PKCs translocate from the cytosol to the cellular membranes, we analysed, by Western blots, the distribution of PKCs expressed by MCF-7 (PKC-α, -δ, -ε, -ι and -ζ [31]) in cells treated with 10 μM Pt(O,O′-acac)(γ-acac)(DMS)] for different incubation times (0.5, 1, 5, and 10 min). As shown in Fig. 8A, a cytosol-to-membrane translocations of PKC-α, PKC-δ and PKC-ε were observed. The involvement of translocating PKCs in the effect of [Pt(O,O′-acac)(γ-acac)(DMS)] on extracellular Ca^{2+} entry was investigated by using the PKC inhibitors GF109203X (able to inhibit all isoforms) and Gö6976 (and inhibitor of conventional, calcium-dependent PKC-α; note that PKC-α is the only conventional PKC expressed by MCF-7 cells) [32]. Pre-incubation of cells with GF109203X (0.1 and 1 μM for 15 min) (data not shown), or with Gö6976 (1 μM) for 15 min, reversed the effects of 10 μM [Pt(O,O′-acac)(γ-acac)(DMS)] on extracellular Ca^{2+} entry (Fig. 8B), suggesting that such effects may be mediated by PKC-α. The role of PKC-α in modulating plasma membrane permeability can also be seen in experiments of Mn^{2+} quenching, where the use of Gö6976 in cells treated with both [Pt(O,O′-acac)(γ-acac)(DMS)] and ATP significantly increased the Mn^{2+} influx (from 5.77 ± 0.22 to 14.70 ± 0.46 Δ_{360}/min, $p < 0.05$; $n = 6$), back to values obtained in cells treated with ATP only (Fig. 8C). Moreover, Gö6976 reversed the effects of [Pt(O,O′-acac)(γ-acac)(DMS)] on plasma membrane permeability in untreated cells (from 2.19 ± 0.13 to 6.52 ± 0.26 Δ_{360}/min, $p < 0.05$; $n = 6$, Fig. 8B). These results suggest that [Pt(O,O′-acac)(γ-acac)(DMS)]-activated PKC-α changed the plasmalemma Ca^{2+} permeability interfering with some Ca^{2+} plasma membrane channels.

3.8. ROS are responsible for the [Pt(O,O′-acac)(γ-acac)(DMS)]-induced decrease of the PMCA activity

[Pt(O,O′-acac)(γ-acac)(DMS)] increased the level of ROS in a time-dependent manner with ROS generation significantly different respect to control (ANOVA: $p < 0.005$) as soon as 1 min (Fig. 9A). [Pt(O,O′-acac)(γ-acac)(DMS)]-provoked ROS production was partially inhibited by diphenyleneiodonium (DPI), an inhibitor of the NADPH oxidase (Fig. 9D). Since another important sources of intracellular ROS are mitochondria, we studied the specific

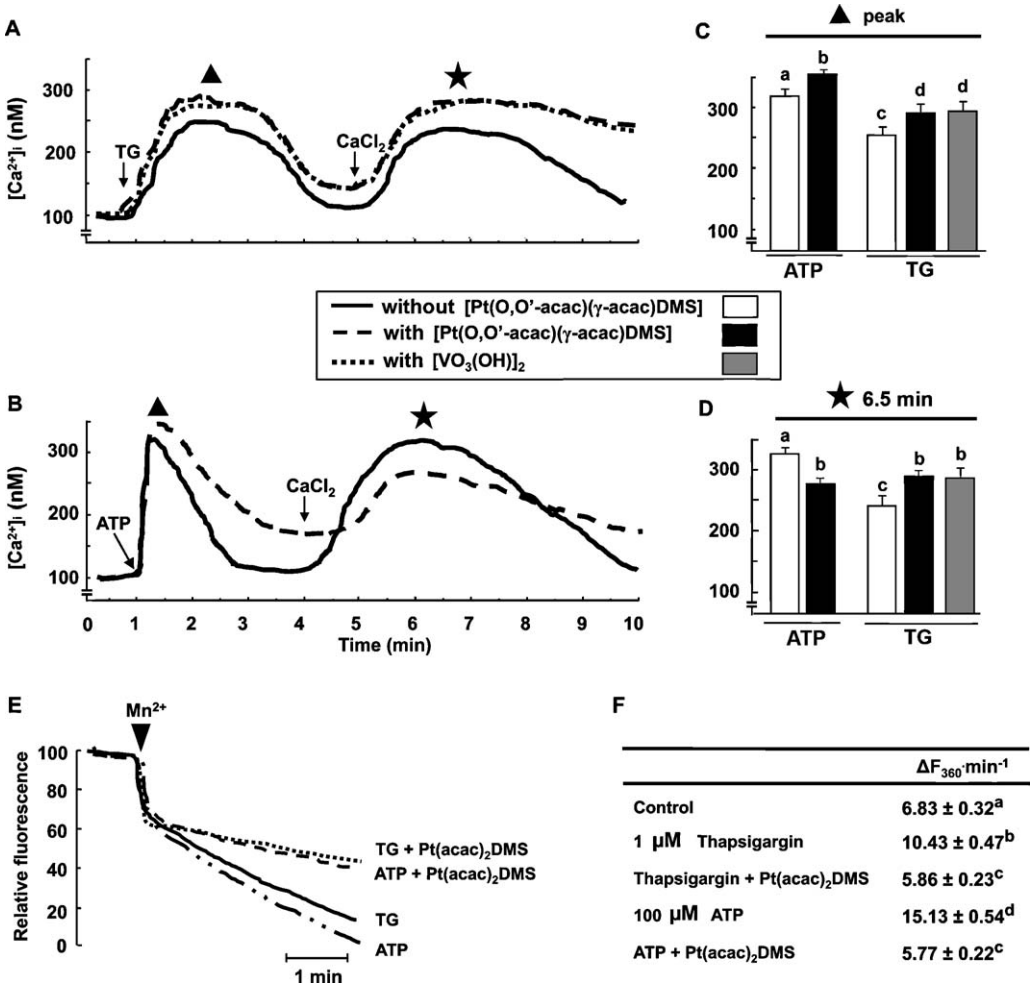

Fig. 6. Effect of [Pt(O,O′-acac)(γ-acac)(DMS)] on extracellular Ca^{2+} entry.
(A) Intracellular Ca^{2+} stores were previously depleted by exposure to 1 μM thapsigargin (TG) in Ca^{2+}-free solution and then 2 mM $CaCl_2$ was added. Extracellular Ca^{2+} entry into MCF-7 cells was evaluated in the absence and in the presence of 10 μM [Pt(O,O′-acac)(γ-acac)(DMS)] or 2 μM orthovanadate ($[VO_3(OH)]_2$).
(B) Effect of 10 μM [Pt(O,O′-acac)(γ-acac)(DMS)] on the extracellular Ca^{2+} entry into MCF-7 cells stimulated with ATP. In nominal Ca^{2+}-free medium, 100 μM ATP was added followed by 2 mM $CaCl_2$ after 4 min in the absence and in the presence of 10 μM [Pt(O,O′-acac)(γ-acac)(DMS)].
(C, D) $[Ca^{2+}]_i$ values obtained from A and B representing the mobilization of internal calcium (peak in C) and the extracellular Ca^{2+} entry ($CaCl_2$) after 6.5 min (in D) of stimulation with ATP or thapsigargin in the presence or absence of [Pt(O,O′-acac)(γ-acac)(DMS)]. The data are means ± S.D. of four different experiments run in triplicate. Values with shared letters are not significantly different according to Bonferroni/Dunn post hoc tests. $Pt(acac)_2DMS$ stands for [Pt(O,O′-acac)(γ-acac)DMS].
(E) Effect of 10 μM [Pt(O,O′-acac)(γ-acac)(DMS)] on thapsigargin- or ATP-induced extracellular Mn^{2+} entry in Ca^{2+}-free solution. After Ca^{2+} store depletion with thapsigargin or ATP, cells were exposed to 2 mM Mn^{2+}, in the presence or in the absence of [Pt(O,O′-acac)(γ-acac)(DMS)]. Each tracing is representative of five separate experiments.
(F) Average data are from experiments shown in (E) ($n = 5$). Values with shared letters are not significantly different according to Bonferroni/Dunn post hoc tests.

production of mitochondrial O^{2-} by MitoSOX red. We found that [Pt(*O,O*′-acac)(γ-acac)(DMS)] increased the mitochondrial synthesis of O^{2-} (Fig. 9B), in a time-dependent manner (Fig. 9C), and that such effect was blocked by the antioxidant apocynin (10 μM). Apocynin also reversed the [Pt(*O,O*′-acac)(γ-acac)(DMS)]-provoked inhibition of PMCA activity (Fig. 9E).

3.9. Effects of [Pt(O,O′-acac)(γ-acac)(DMS)] on other human breast cell lines

To determine whether the observations made on MCF-7 cells are also valid for other cell lines, we tested two other breast cancer cell lines, MDA-MB-231 and SKBR-3. Furthermore, we also included the MCF-10A, a nontumorigenic breast epithelial cell that appeared to be less sensitive to [Pt(*O,O*′-acac)(γ-acac)(DMS)] than MCF-7 cells in cytotoxicity assays [16]. Thus, a selected set of crucial experiments (effects of 10 μM [Pt(*O,O*′-acac)(γ-acac)(DMS)] on (a) intracellular $[Ca^{2+}]_i$ levels, (b) membrane permeability, (c) PMCA activity and (d) ROS generation)) were performed and the results shown in Table 1. The results show that the effect of [Pt(*O,O*′-acac)(γ-acac)(DMS)] are not significantly different in the three tumor cell lines while, on the contrary, such effects are much less evident, although significant compared with controls, in normal MCF-10A cells.

4. Discussion

Antineoplastic drugs resistance poses a major impediment to the successful treatment of breast cancer. About 70% of breast cancers are oestrogen receptor positive (ER+ve). The remaining 30% are ER−ve [33]. Oestrogen hormone promotes breast cancer cell proliferation through ER, therefore, oestrogen antagonists such as tamoxifen are used to block ER activation in ER+ve breast cancer patients [34]. We have previously synthesized a new Pt complex, [Pt(O,O′-acac)(γ-acac)(DMS)], in the attempt to find novel strategies for a better management of ER-ve breast cancer. This compound may be a promising new therapeutic agent because it induces apoptosis in MCF-7 breast cancer cell line, relatively

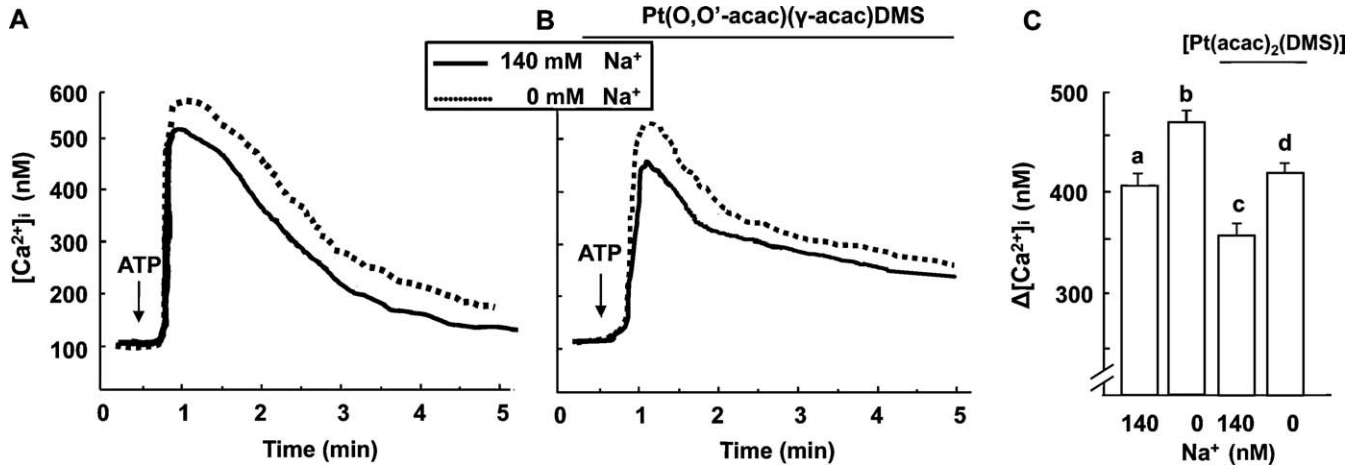

Fig. 7. Effects of [Pt(O,O′-acac)(γ-acac)(DMS)] on Na^+/Ca^{2+}-Exchanger activity.
(A) Ca^{2+} influx in cells stimulated with ATP, in buffers with Na^+ concentrations of 0 and 140 nM, in the presence (B) or not (A) of [Pt(O,O′-acac)(γ-acac)(DMS)]. Results shown are representative of four different experiments.
(C) $\Delta[Ca^{2+}]_i$ values obtained from A and B after 30 s (peak) stimulation with ATP in normal and Na^+-free buffers in the presence or not of [Pt(O,O′-acac)(γ-acac)(DMS)]. The data are means ± S.D. of four different experiments run in triplicate. Values with shared letters are not significantly different according to Bonferroni/Dunn post hoc tests. $Pt(acac)_2$DMS stands for [Pt(O,O′-acac)(γ-acac)DMS].

insensitive to cisplatin [16]. We have demonstrated that [Pt(O,O′-acac)(γ-acac)(DMS)] decreases Bcl-2 expression in MCF-7 cells and contributes to the formation of pores by facilitating the translocation of Bax, a proapoptotic factor, from the cytosol to the outer mitochondrial membrane [16]. This mechanism, allows the dissipation of mitochondrial membrane potential and the release of cytochrome c and is Ca^{2+} independent [35]. Furthermore, the dissipation of membrane potential minimizes the contribution of mitochondria to Ca^{2+} homeostasis and causes ATP depletion which further increases the $[Ca^{2+}]_i$ by decreasing the Ca^{2+} pump activities. It is well known that in apoptosis, the appropriateness of Ca^{2+} handling is of fundamental importance [4] with Ca^{2+} playing different roles in this process; for example, Ca^{2+} from the extracellular space, or released from endoplasmic reticulum, leads

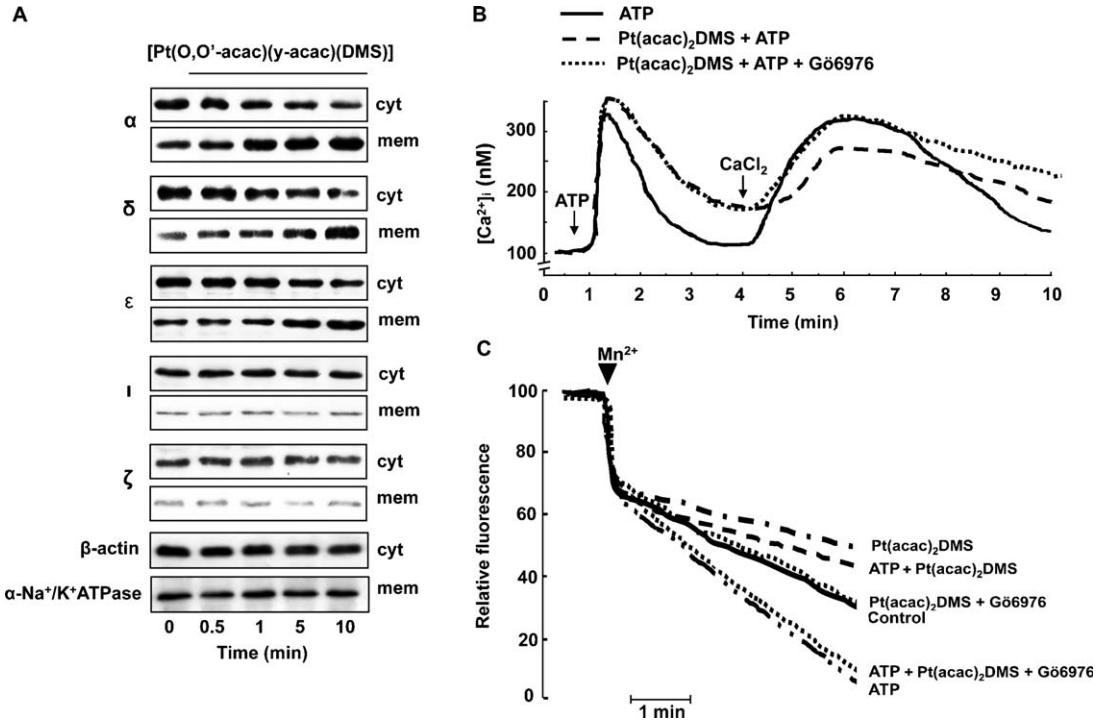

Fig. 8. The effect of [Pt(O,O′-acac)(γ-acac)(DMS)] on extracellular Ca^{2+} entry is due to PKC-α activation.
(A) MCF-7 cells were treated without or with 10 μM [Pt(O,O′-acac)(γ-acac)(DMS)] for the indicated times. Cytosol (cyt) and membrane (mem) fractions for translocation studies, were analyzed by western blotting with specific anti-PKCs antibodies. The purity of fractions was tested by immunoblotting with anti β-actin and anti-α subunit of Na^+/K^+ATPase monoclonal antibodies. The figures are representative of four independent experiments.
(B, C) MCF-7 cells, loaded with fura-2-AM, and kept in nominally Ca^{2+}-free medium, were stimulated with ATP or ATP plus 10 μM [Pt(O,O′-acac)(γ-acac)(DMS)], with or without 1 μM Gö 6976. (C) Mn^{2+} entry was measured by the quenching of fluorescence with an excitation wavelength of 360 nm, and an emission wavelength of 510 nm. The curves represent fluorescence relative to total quenching attained by the addition of digitonin to saturate fura-2 with Mn^{2+}. Each tracing is representative of six separate experiments.
Arrows indicate time points at which 100 μM ATP, 2 mM $CaCl_2$ or 2 mM Mn^{2+} were added. $Pt(acac)_2$DMS stands for [Pt(O,O′-acac)(γ-acac)DMS].

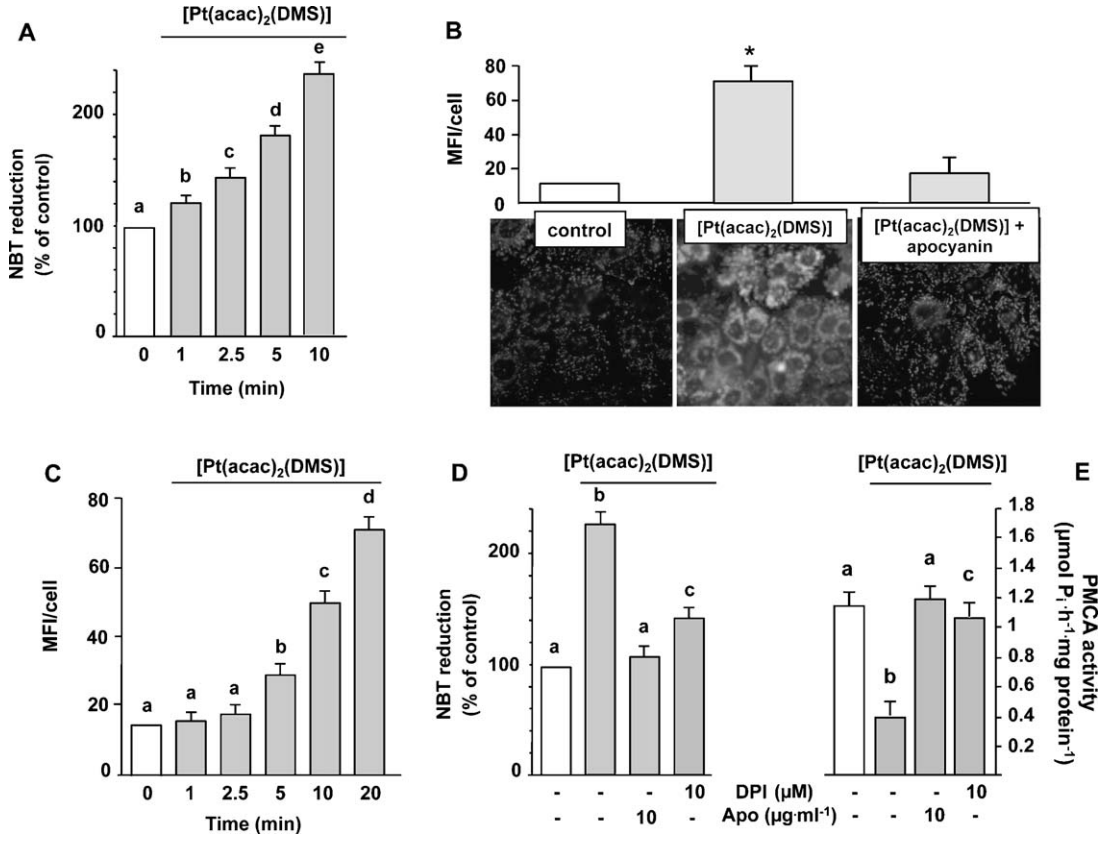

Fig. 9. The effect of [Pt(O,O′-acac)(γ-acac)(DMS)] on PMCA is due to Reactive Oxygen Species (ROS) generation.
(A) Cells were treated or not with 10 μM [Pt(O,O′-acac)(γ-acac)(DMS)] for the indicated time intervals. ROS production was assayed by NBT reduction as described in Section 2. The data are means ± S.D. of four different experiments. Values with shared letters are not significantly different according to Bonferroni/Dunn post hoc tests.
(B) Cells were treated or not with 10 μM [Pt(O,O′-acac)(γ-acac)(DMS)] and with or without apocynin for 20 min and superoxide anion production was determined by MitoSOX staining in fluorescence microscopy. Lower panel shows the increase in superoxide production induced by [Pt(O,O′-acac)(γ-acac)(DMS)] by fluorescence microscopy. The mean fluorescence intensities (MFI/cell) ± S.D. are shown in upper panel ($n = 4$; $^{*}p \leq 0.001$).
(C) Time-response experiments with 10 μM [Pt(O,O′-acac)(γ-acac)(DMS)] showing the increase of MitoSOX Red fluorescence induced by [Pt(O,O′-acac)(γ-acac)(DMS)]. Results are expressed in MFI/cell ± S.D. of four different experiments.
(D, E) Cells preincubated with or without apocynin (Apo) or diphenyleneiodonium (DPI) for 30 min were exposed to 10 μM [Pt(O,O′-acac)(γ-acac)(DMS)] for 10 min. ROS production and PMCA activity were assayed as described in Section 2. The data are means ± S.D. of four different experiments. Values with shared letters are not significantly different according to Bonferroni/Dunn post hoc tests. $Pt(acac)_2DMS$ stands for [Pt(O,O′-acac)(γ-acac)DMS].

to an increase in the mitochondrial Ca^{2+} concentration, which results in the increase of transition pore permeability which activates apoptosis [6]. It is well established that altered expression of specific Ca^{2+} channels and pumps are characteristic features of some cancers and anticancer drugs such as cisplatin, are able to increase $[Ca^{2+}]_i$ through various mechanisms [36–38]. We here show that [Pt(O,O′-acac)(γ-acac)(DMS)] evokes an early increase in $[Ca^{2+}]_i$ (Fig. 1A). This supports the hypothesis that homeostatic mechanisms involved in the regulation of $[Ca^{2+}]_i$ may play a role during [Pt(O,O′-acac)(γ-acac)(DMS)]-induced apoptosis. The increase of $[Ca^{2+}]_i$ provoked by [Pt(O,O′-acac)(γ-acac)(DMS)] does not depend on the external Ca^{2+} concentration (Figs. 5 and 6). Indeed, [Pt(O,O′-acac)(γ-acac)(DMS)] decreased the permeability of the plasma membrane, an effect that is comparable to that caused by La^{3+} (Fig. 2). This increase could be caused by the action of [Pt(O,O′-acac)(γ-acac)(DMS)] on at least one of the various systems that regulate Ca^{2+} homeostasis, such as Ca^{2+} transport pumps (the plasma membrane Ca^{2+}-ATPases PMCAs, the sarco/endoplasmic reticulum Ca^{2+}-ATPases SERCAs, and the secretory pathway Ca^{2+}-ATPases SPCAs), and secondary Na^{+}/Ca^{2+}

Table 1
Effects of Pt(O,O′-acac)(γ-acac)(DMS)] in human breast cell lines.

	MCF-7	SKBR-3	MDA-MB-231	MCF-10A
$\Delta[Ca^{2+}]_i$	151 ± 15^a	128 ± 13^a	132 ± 17^a	18 ± 4^b
$\Delta F_{360}\,min^{-1}$	-64 ± 9^a	-53 ± 7^a	-48 ± 7^a	-22 ± 3^b
ΔPMCA activity	-75 ± 11^a	-62 ± 9^a	-66 ± 8^a	-28 ± 2^b
ΔNBT reduction	140 ± 13^a	122 ± 11^a	113 ± 9^a	21 ± 5^b

$\Delta[Ca^{2+}]_i$ represents the increase in free intracellular calcium concentration, obtained by fluorimetry using Fura-2, in cell incubated with 10 μM Pt(O,O′-acac)(γ-acac)(DMS)] for 20 min.
ΔF360min-1 represents the decrease of the plasma membrane permeability to Mn^{2+} influx after the addition of 10 μM [Pt(O,O′-acac)(γ-acac)(DMS)].
ΔPMCA represents the decrease in the ATPase activity of the PMCA in cells incubated with 10 μM Pt(O,O′-acac)(γ-acac)(DMS)] for 10 min.
ΔNBT represent the increase in ROS generation obtained by nitroblue tetrazolium (NBT) assay in cells incubated with 10 μM Pt(O,O′-acac)(γ-acac)(DMS)] for 10 min.
Results are expressed as the percentage ratio over control cells.The data are means ± S.D. of four different experiments. Values with shared letters are not significantly different according to Bonferroni/Dunn post hoc tests.

antiporter. We have shown that both SPCA and SERCA activities were not affected by the treatment with [Pt(O,O′-acac)(γ-acac)(DMS)] (Fig. 3). The PMCA removes the Ca^{2+} through the plasma membrane and is important for the maintenance of basal levels of cytosolic Ca^{2+} and lowering of $[Ca^{2+}]_i$ after the generation of Ca^{2+} transients [1]. Measuring the ATPase activity gave a direct indication that PMCA was inhibited by Pt(O,O′-acac)(γ-acac)(DMS)] (Fig. 3). This inhibition resulted in changes in the ATP-induced $[Ca^{2+}]_i$ profile. These changes are clearly due mainly to the combined effects of [Pt(O,O′-acac)(γ-acac)(DMS)] on permeability and PMCA activity. Since the effects of inhibition of PMCA occurred slowly (Fig. 3C), compared to changes in permeability (Figs. 2, 6E and 8C), these latter changes became more important in the second phase of the transient, causing an overall rise in Ca^{2+} level. Clearly, PMCA represents a potential therapeutic target, since its inhibition affects the efflux of Ca^{2+} by increasing its concentration that may eventually lead to the induction of apoptosis. In this regard it has been shown that even the partial inhibition of PMCA-mediated Ca^{2+} efflux is sufficient to reduce proliferation of MCF-7 cells [38]. Furthermore, an antisense construct directed towards PMCA leads to changes in cell-cycle kinetics, such as lengthening the G2 phase and simultaneously reducing the Ca^{2+} efflux [39]. PMCA is a very sensitive target for oxidative stress as occurs in pancreatic acinar cells [40] and in neuronal and liver membranes [41,42]. We have noticed that addition of [Pt(O,O′-acac)(γ-acac)(DMS) to MCF-7 cells induces rapid production of ROS (Fig. 9A and C). It is known that ROS can be produced through the activation of NAD(P)H oxidase, or mitochondrial pathways [43]. Therefore, it is expected that the origin of the ROS in cells treated with [Pt(O,O′-acac)(γ-acac)(DMS)] is twofold: primarily by NAD(P)H oxidase, but also by mitochondria (with apocinyn inhibiting this effect, Fig. 9B). In fact, whilst the inhibition of NAD(P)H oxidase by DPI only partially prevented [Pt(O,O′-acac)(γ-acac)(DMS)]-induced ROS generation, the use of the antioxidant apocinyn inhibited this effect (Fig. 9D) and restored the PMCA activity due to ROS production (Fig. 9E). The effects of ROS on PMCA could be due to either the aggregation of PMCA molecules, as a result of Cys oxidation to disulphides and increased hydrophobic interactions [41], or to the increase of $[Ca^{2+}]_i$ due to the oxidative stress which activates Ca^{2+}-dependent proteases, such as caspases, known to make PMCA inactive [44,45]. A somewhat similar mechanism has been described in neurons, whereby cleavage of the Na^+/Ca^{2+} exchanger by caspases was shown to mediate the Ca^{2+} overload during the excitotoxicity associated with brain ischemia [46]. However, we show that the effects of [Pt(O,O′-acac)(γ-acac)(DMS)] on $[Ca^{2+}]_i$ are not due to modulation of the Na^+/Ca^{2+} exchanger activity (Fig. 7). It seems that the mechanism dependent on caspase activation does not occur in our case. This conclusion is based upon previous results [16] which show that the time frame over which caspases became significantly activated by [Pt(O,O′-acac)(γ-acac)(DMS)] occurred much later compared to the inactivation of PMCA, which is already evident after 30-s exposure to [Pt(O,O′-acac)(γ-acac)(DMS)] (Fig. 3C). Consequently, the anti-neoplastic potential of [Pt(O,O′-acac)(γ-acac)(DMS)] might also be based on its ability to produce changes in Ca^{2+} homeostasis, like others pump inhibitors. We have tried to estimate the possible effect of [Pt(O,O′-acac)(γ-acac)(DMS)] on the membrane permeability to Ca^{2+}. A raise in the $[Ca^{2+}]_i$ can be due to Ca^{2+}-influx from the extracellular space or Ca^{2+}-release from intracellular stores [5,47]. Channels mediating Ca^{2+}-influx from the extracellular space are voltage-gated and ligand-gated channels, TRP and store-operated channels. In general, non-excitable tissues, including the epithelium, do not express voltage gated Ca^{2+} channels. However, recent studies have shown that T-type Ca^{2+} channels are expressed in cancerous cells, MCF-7 included [48]. MCF-7 cells also express TRPM7 [49] and 8 [50], TRC1 [51] and 6 [52]. TRPV6 is an endothelial calcium entry channel that is strongly expressed in breast adenocarcinoma tissue [7], suggesting that it may play some role in tumor development. Tamoxifen inhibits TRPV6 activity in TRPV6-expressing MCF-7 breast cancer cells [53] and alters Ca^{2+} signalling in MCF-7 breast cancer cells. In malignant glioma cell lines tamoxifen increases cytosolic Ca^{2+} responses to ATP-agonist activation [13]. Some metals (e.g. Pb^{2+} [54] and methyl-mercury [55]), directly block membrane channels leading to a decrease in $[Ca^{2+}]_i$. [Pt(O,O′-acac)(γ-acac)(DMS)] reduced the Ca^{2+}-influx from the extracellular space, as demonstrated by the fluorescence quenching due to Mn^{2+} influx (Figs. 2 and 6E). Mn^{2+} enters the cell using Ca^{2+} channels but it is neither transported by either the SERCA nor by PMCA. [Pt(O,O′-acac)(γ-acac)(DMS)] decreases the entry of Mn^{2+} in cells untreated (Fig. 2) and treated with either ATP or thapsigargin (Fig. 6E). Since the effects were greatest in ATP-treated cells, it is likely that [Pt(O,O′-acac)(γ-acac)(DMS)] acts also on channels coupled to G proteins or second messengers produced by agonists such as ATP. In this regard, it is known that the PKCs are intracellular transducers also involved in regulating Ca^{2+} influx [30]. PKC-α is the first isoform activated in [Pt(O,O′-acac)(γ-acac)(DMS)]-treated cells. This activation is temporally compatible with the rapid decrease in the plasmamembrane permeability (Fig. 8A). The involvement of PKC-α is highlighted by the effects elicited by its pharmacological inhibition (Fig. 8B and C). Contrary to other metals, [Pt(O,O′-acac)(γ-acac)(DMS)] does not interact directly with channels but it activates intracellular signalling leading to the control of some Ca^{2+} channels. We wanted to investigate if the effects of [Pt(O,O′-acac)(γ-acac)(DMS)] on Ca^{2+} homeostasis also had an impact on the cell ability to handle the complex changes during Ca^{2+} signalling evoked by extracellular stimuli. To this end, we studied the effects of [Pt(O,O′-acac)(γ-acac)(DMS)] on the strong disturbance in Ca^{2+} levels obtained by stimulating the purinergic receptor. ATP-induced Ca^{2+} response was characterized by two distinct components: an initial rapid and transient rise of $[Ca^{2+}]_i$, predominantly originating from the endoplasmic reticulum through inositol 1,4,5-trisphosphate receptor (InsP3) receptors (InsP3Rs), and a sustained phase due to Ca^{2+} influx from the extracellular space (Fig. 4A). The latter was previously characterized as extracellular Ca^{2+} entry in response to depletion of the ER Ca^{2+} stores [24,25]. Ca^{2+} ions transients evoked by ATP were effectively reduced by [Pt(O,O′-acac)(γ-acac)(DMS)], both in the values of the spikes and, especially, in those of the sustained phase of elevated $[Ca^{2+}]_i$ (Fig. 4B). Experiments with La^{3+}, a Ca^{2+} channel blocker that has no effects on PMCA activity, corroborated the idea that the changing in the ATP-provoked $[Ca^{2+}]_i$ profile due to [Pt(O,O′-acac)(γ-acac)(DMS)], were due to PMCA activity inhibition and plasma membrane channels closure (Fig. 4B, C and D). The involvement of these channels, and the importance of PMCA inhibition, was observed in experiments performed with ATP in buffer without Ca^{2+}, where [Pt(O,O′-acac)(γ-acac)(DMS)] increased slightly, but significantly, the ATP-provoked Ca^{2+} transient (Fig. 5A and C). This increase may be due to the inhibition of PMCA. We noticed that the addition of external Ca^{2+} causes a significant extracellular Ca^{2+} entry that is in part blocked by [Pt(O,O′-acac)(γ-acac)(DMS)] (Figs. 5 and 6). [Pt(O,O′-acac)(γ-acac)(DMS)] does not seem to affect the Ca^{2+} released from the intracellular stores because no significant effect on Ca^{2+} transient provoked by ATP was evident in cells with the InsP3Rs blocked by 2-APB (with the exception of a slight increase in the plateau). This may also be due to the decreased PMCA activity (Fig. 5B and C). Consistently, [Pt(O,O′-acac)(γ-acac)(DMS)] had effect on Ca^{2+} peak provoked by ATP in Ca^{2+}-free buffers and on the $[Ca^{2+}]_i$ returning to control values, a phase that resulted to be slower due to reduced calcium efflux (Fig. 6B and C). Finally, it is important to note that the results we obtained (Table 1) on the

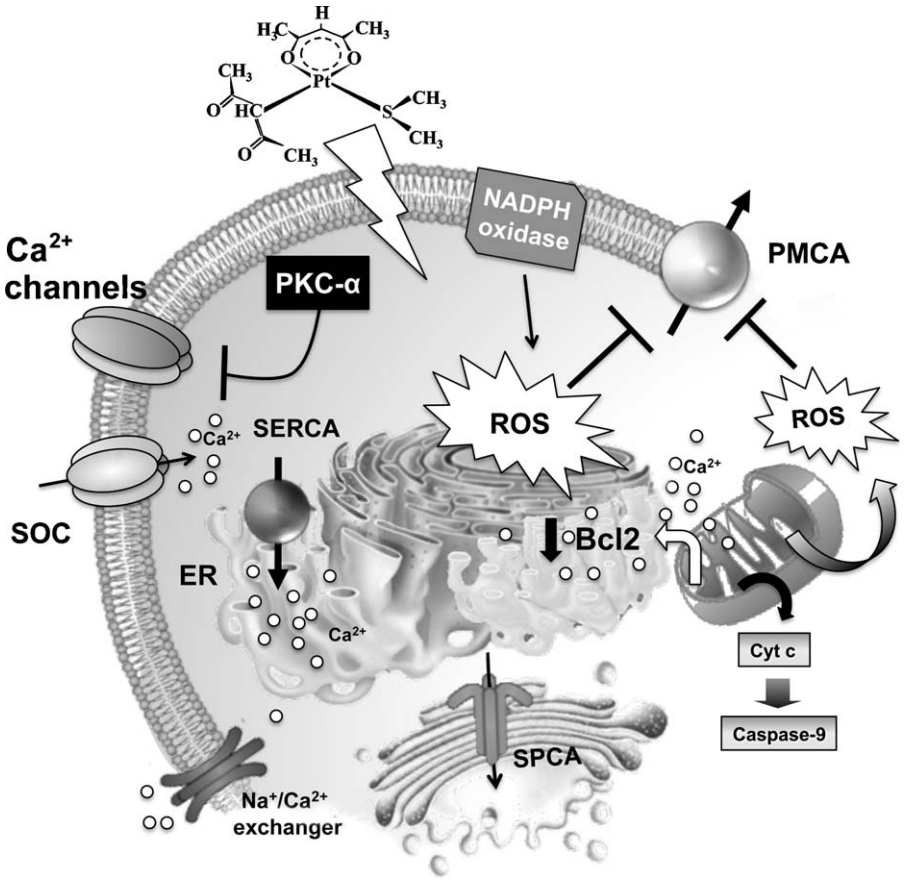

Fig. 10. Mechanisms of Pt(O,O′-acac)(γ-acac)(DMS)]-induced apoptosis.
Pt(O,O′-acac)(γ-acac)(DMS)] alters the $[Ca^{2+}]_i$; this change is due both to the PKC-α-mediated closure of some channels and, primarily, to the decrease of PMCA activity, due to NADPH oxidase and mitochondrial ROS production.
Previous results [16] demonstrated that Pt(O,O′-acac)(γ-acac)(DMS)] targets the mitochondria, resulting in dissipation of the membrane potential that may minimize the contribution of mitochondria to Ca^{2+} homeostasis. Subsequent mitochondrial release of cyt c leads to activation of caspase-9, resulting in apoptosis. Pt(O,O′-acac)(γ-acac)(DMS)] also decreased Bcl-2 expression thus diminuishing its contribution to the endoplasmic reticulum Ca^{2+} uptake, an effect likely related to its anti-apoptotic function.

various breast cell lines provide evidence that [Pt(O,O′-acac)(γ-acac)(DMS)] may be a promising new anticancer agent, as it exhibited higher calcium homeostasis perturbation in cancer cell lines than in non-cancerous MCF-10A cells, which also appeared to be less sensitive to the cytotoxic effect of the Pt-compound [16].

In conclusion, we demonstrated that [Pt(O,O′-acac)(γ-acac)(DMS)] alters the $[Ca^{2+}]_i$ and that this change is due both to the PKC-α-mediated closure of some channels and to the inhibition of PMCA. The key points of this model are summarized in Fig. 10. The overall effect of [Pt(O,O′-acac)(γ-acac)(DMS)] is to increase the $[Ca^{2+}]_i$, an effect that is linked to its ability to trigger rapid apoptosis in MCF-7 cells.

Conflict of interest

The authors state no conflict of interest.

Acknowledgement

The research was supported by University of Salento (Fondi di Ateneo per la Ricerca di Base, 2009).

References

[1] Carafoli E, Santella L, Branca D, Brini M. Generation, control, and processing of cellular calcium signals. Crit Rev Biochem Mol Biol 2001;36:107–260.
[2] Lipskaia L, Lompré AM. Alteration in temporal kinetics of Ca^{2+} signaling and control of growth and proliferation. Biol Cell 2004;96:55–68.
[3] Kahl CR, Means AR. Regulation of cell cycle progression by calcium/calmodulin-dependent pathways. Endocr Rev 2003;24:719–36.
[4] Orrenius S, Zhivotovsky B, Nicotera P. Regulation of cell death: the calcium-apoptosis link. Nat Rev Mol Cell Biol 2003;4:552–65.
[5] Berridge MJ, Bootman MD, Roderick HL. Calcium signalling: dynamics, homeostasis and remodelling. Nat Rev Mol Cell Biol 2003;4:517–29.
[6] Rizzuto R, Pozzan T. When calcium goes wrong: genetic alterations of a ubiquitous signaling route. Nat Genet 2003;34:135–41.
[7] Zhuang L, Peng JB, Tou L, Takanaga H, Adam RM, Hediger Ma, et al. Calcium-selective ion channel, CaT1, is apically localized in gastrointestinal tract epithelia and is aberrantly expressed in human malignancies. Lab Invest 2002;82:1755–64.
[8] Kamrava MR, Michener CM, Kohn EC. Calcium signaling as a molecular target in cancer. Pharm News 2002;9:435–42.
[9] Lee WJ, Roberts-Thomson SJ, Holman NA, May FJ, Lehrbach GM, Monteith GR. Expression of plasma membrane calcium pump isoform mRNAs in breast cancer cell lines. Cell Signal 2002;14:1015–22.
[10] Reisner PD, Brandt PC, Vanaman TC. Analysis of plasma membrane Ca 2+-ATPase expression in control and SV40-transformed human fibroblasts. Cell Calcium 1997;21:53–62.
[11] Chene P. ATPases as drug targets: learning from their structure. Nat Rev Drug Discov 2002;1:665–73.
[12] Johnson PH, Walker RP, Jones SW, Stephens K, Meurer J, Zajchowski. et al. Multiplex gene expression analysis for high-throughput drug discovery: screening and analysis of compounds affecting genes overexpressed in cancer cells. Mol Cancer Ther 2002;1:1293–304.
[13] Zhang W, Couldwell WT, Song H, Takano T, Lin JHC, et al. Tamoxifen-induced enhancement of calcium signaling in glioma and MCF-7 breast cancer cells. Cancer Res 2000;60:5395–400.
[14] De Pascali SA, Papadia P, Ciccarese A, Pacifico C, Fanizzi FP. First examples of β-diketonate platinum II complexes with sulfoxide ligands. Eur J Inorg Chem 2005;5:788–96.

[15] Muscella A, Calabriso N, De Pascali SA, Urso L, Ciccarese A, Fanizzi FP, et al. New platinum II complexes containing both an O,O′-chelated acetylacetonate ligand and a sulfur ligand in the platinum coordination sphere induce apoptosis in HeLa cervical carcinoma cells. Biochem Pharmacol 2007;74:28–40.
[16] Muscella A, Calabriso N, Fanizzi FP, De Pascali SA, Urso L, Ciccarese A, et al. [Pt O,O′-acac γ-acac DMS], a new Pt compound exerting fast cytotoxicity in MCF-7 breast cancer cells via the mitochondrial apoptotic pathway. Br J Pharmacol 2008;153:34–49.
[17] Grynkiewicz G, Poenie M, Tsien RY. A new generation of calcium indicators with greatly improved fluorescence properties. J Biol Chem 1985;260:3440–50.
[18] Higgins JA. Separation and analysis of membrane lipid components. In: Findlay JBC, Evans WH, editors. Biological membranes, a practical approach. Oxford: IRL Press; 1987. p. 103–37.
[19] Lytton J, Westlin M, Hanley MR. Thapsigargin inhibits the sarcoplasmic and endoplasmic reticulum Ca^{2+}-ATPase family of calcium pumps. J Biol Chem 1991;266:17067–71.
[20] Sepúlveda MR, Berrocal M, Marcos D, Wuytack F, Mata AM. Functional and immunocytochemical evidence for the expression and localization of the secretory pathway Ca^{2+}-ATPase isoform 1 SPCA1 in cerebellum relative to other Ca^{2+} pumps. J Neurochem 2007;103:1009–18.
[21] Gatto C, Hale CC, Xu W, Milanick MA. Eosin, a potent inhibitor of the plasma membrane Ca pump, does not inhibit the cardiac Na-Ca exchanger. Biochemistry 1995;34:965–72.
[22] Muscella A, Calabriso N, Vetrugno C, Urso L, Fanizzi FP, De Pascali SA, et al. Sublethal concentrations of the platinum II complex [Pt O,O′-acac γ-acac DMS] alter the motility and induce anoikis in MCF-7 cells. Br J Pharmacol 2010;160:1362–77.
[23] Merritt JE, Hallam TJ. Platelets and parotid acinar cells have different mechanisms for agonist-stimulated divalent cation entry. J Biol Chem 1998;263: 6161–6164.
[24] Muscella A, Greco S, Elia MG, Storelli C, Marsigliante S. Angiotensin II stimulation of Na+/K+ATPase activity and cell growth by calcium-independent pathway in MCF-7 breast cancer cells. J Endocrinol 2002;173:315–23.
[25] Bowler WB, Dixon CJ, Halleux C, Maier R, Bilbe G, Fraser WD, et al. Signalling in human osteoblasts by extracellular nucleotides-their weak induction of the c-Fos proto-oncogene via Ca^{2+} mobilisation is strongly potentiated by a parathyroid hormone/cAMP-dependent protein kinase pathway independently of mitogen-activated protein kinase. J Biol Chem 1999;274:14315–24.
[26] Rossi AM, Picotto G, de Boland AR, Boland RL. Evidence on the operation of ATP-induced capacitative calcium entry in breast cancer cells and its blockade by 17beta-estradiol. J Cell Biochem 2002;87:324–33.
[27] Maruyama T, Kanaji T, Nakade S, Kanno T, Mikoshiba K. 2APB, 2-aminoethoxydiphenyl borate, a membrane-penetrable modulator of Ins 1,4,5 P3-induced Ca^{2+} release. J Biochem 1997;122:498–505.
[28] Peppiatt CM, Collins TJ, Mackenzie L, Conway SJ, Holmes AB, Bootman MD, et al. 2-Aminoethoxydiphenyl borate 2-APB antagonises inositol 1,4,5-trisphosphate-induced calcium release, inhibits calcium pumps and has a use-dependent and slowly reversible action on store-operated calcium entry channels. Cell Calcium 2003;34:97–108.
[29] Anantamongkol U, Takemura H, Suthiphongchai T, Krishnamra N, Horio Y. Regulation of Ca^{2+} mobilization by prolactin in mammary gland cells: possible role of secretory pathway Ca^{2+}-ATPase type 2. Biochem Biophys Res Commun 2007;352:537–42.
[30] McHugh D, Sharp EM, Scheuer T, Catterall WA. Inhibition of cardiac L-type calcium channels by protein kinase C phosphorylation of two sites in the N-terminal domain. Proc Natl Acad Sci USA 2000;97:12334–8.
[31] Muscella A, Greco S, Elia MG, Storelli C, Marsigliante S. PKC-zeta is required for angiotensin II-induced activation of ERK and synthesis of C-FOS in MCF-7 cells. J Cell Physiol 2003;197:61–8.
[32] Qatsha KA, Rudolph C, Marme D, Schachtele C, May WS. Gö 6976, a selective inhibitor of protein kinase C, is a potent antagonist of human immunodeficiency virus 1 induction from latent/low-level-producing reservoir cells in vitro. Proc Natl Acad Sci USA 1993;90:4674–8.
[33] Osborne CK, Yochmowitz MG, Knight 3rd WA, McGuire WL. The value of estrogen and progesterone receptors in the treatment of breast cancer. Cancer 1980;46:2884–8.
[34] Thorpe SM. Estrogen and progesterone receptor determinations in breast cancer, technology, biology and clinical significance. Acta Oncol 1988; 27:1–19.
[35] Wei MC, Zong WX, Cheng EH, Lindsten T, Panoutsakopoulou V, Ross AJ, et al. Proapoptotic BAX and BAK: a requisite gateway to mitochondrial dysfunction and death. Science 2001;292:727–30.
[36] Florea AM, Büsselberg D. Occurrence, use and potential toxic effects of metals and metal compounds. Biometals 2006;19:419–27.
[37] Tomaszewski, Büsselberg D. SnCl2 reduces voltage-activated calcium channel currents of dorsal root ganglion neurons of rats. Neurotoxicology 2008;29:958–63.
[38] Kawai Y, Nakao T, Kunimura N, Kohda Y, Gemba M. Relationship of intracellular calcium and oxygen radicals to cisplatin-related renal cell injury. J Pharmacol Sci 2006;100:65–72.
[39] Lee W, Robinson JA, Holman NA, McCall MN, Roberts-Thomson SJ, Monteith GR. Antisense-mediated inhibition of the plasma membrane calcium-ATPase suppresses proliferation of MCF-7 cells. J Biol Chem 2005;280: 27076–27084.
[40] Pariente JA, Camello C, Camello PJ, Salido GM. Release of calcium from mitochondrial and non mitochondrial intracellular stores in mouse pancreatic acinar cells by hydrogen peroxide. J Membr Biol 2001;179:27–35.
[41] Zaidi A, Michaelis ML. Effects of reactive oxygen species on brain synaptic plasma membrane Ca^{2+}-ATPase. Free Radic Biol Med 1999;27:810–21.
[42] Bruce JIE, Elliott AC. Oxidant-impaired intracellular Ca^{2+} signaling in pancreatic acinar cells: role of the plasma membrane Ca^{2+}-ATPase. Am J Physiol Cell Physiol 2007;293:C938–50.
[43] Fariss MW, Chan CB, Patel M, Van Houten B, Orrenius S. Role of mitochondria in toxic oxidative stress. Mol Interv 2005;5:94–111.
[44] Pászty K, Antalffy G, Hegedüs L, Padányi R, Penheiter AR, Filoteo AG, et al. Cleavage of the plasma membrane Ca^{2+} ATPase during apoptosis. Ann N Y Acad Sci 2007;1099:440–50.
[45] Schwab BL, Guerini D, Didszun C, Bano D, Ferrando-May E, Fava E, et al. Cleavage of plasma membrane calcium pumps by caspases: a link between apoptosis and necrosis. Cell Death Differ 2002;9:818–31.
[46] Bano D, Young KW, Guerin CJ, Lefeuvre R, Rothwell NJ, Naldini L, et al. Cleavage of the plasma membrane Na^+/Ca^{2+} exchanger in excitotoxicity. Cell 2005;120:275–85.
[47] Clapham DE. Calcium signaling. Cell 2007;131:1047–58.
[48] Taylor JT, Huang L, Pottle JE, Liu K, Yang Y, Zeng X, et al. Selective blockade of T-type Ca^{2+} channels suppresses human breast cancer cell proliferation. Cancer Lett 2008;267:116–24.
[49] Guilbert A, Gautier M, Dhennin-Duthille I, Haren N, Sevestre H, Ouadid-Ahidouch H. Evidence that TRPM7 is required for breast cancer cell proliferation. Am J Physiol Cell Physiol 2009;297:493–502.
[50] Chodon D, Guilbert A, Dhennin-Duthille I, Gautier M, Telliez MS, Sevestre H, et al. Estrogen regulation of TRPM8 expression in breast cancer cells. BMC Cancer 2010;10:212–9.
[51] El Hiani Y, Ahidouch A, Lehen'kyi V, Hague F, Gouilleux F, Mentaverri R, et al. Extracellular signal-regulated kinases 1 and 2 and TRPC1 channels are required for calcium-sensing receptor-stimulated MCF-7 breast cancer cell proliferation. Cell Physiol Biochem 2009;23:335–46.
[52] Guilbert A, Dhennin-Duthille I, Hiani YE, Haren N, Khorsi H, Sevestre H, et al. Expression of TRPC6 channels in human epithelial breast cancer cells. BMC Cancer 2008;8:125–9.
[53] Bolanz KA, Kovacs GG, Landowski CP, Hediger MA. Tamoxifen inhibits TRPV6 activity via estrogen receptor-independent pathways in TRPV6-expressing MCF-7 breast cancer cells. Mol Cancer Res 2009;7:2000–10.
[54] Büsselberg D. Actions of metals on membrane channels, calcium homeostasis and synaptic plastivity. In: Hirner AV, Emons H, editors. Organometal and metalloid specism in the environment: analysis, distribution, processes and toxicological evaluation. Wien, New York: Springer; 2004. p. 259–81.
[55] Leonhardt R, Pekel M, Platt B, Haas HL, Busselberg D. Voltage-activated calcium channel currents of rat DRG neurons are reduced by mercuric chloride $HgCl_2$ and methylmercury CH_3HgCl. Neurotoxicology 1996;17:85–92.